JIMMA UNIVERSITY

SCHOOL OF GRADUATE STUDIES

JIMMA INSTITUTE OF TECHNOLOGY

FACULTY CIVIL AND ENVIRONMENTAL ENGINEERING

STRUCTURAL ENGINEERING STREAM

CONSTRUCTION OF UNIAXIAL INTERACTION DIAGRAM FOR SLENDER REINFORCED CONCRETE COLUMN USING NON LINEAR FE ANALYSIS SOFTWARE

A Thesis Submitted to Graduate Studies of Jimma University in Partial Fulfillment of the Requirements for the Degree of Master Science in Structural Engineering.

By: BEDASO AHMED

Nov, 2018

JIMMA, ETHIOPIA

JIMMA UNIVERSITY

SCHOOL OF GRADUATE STUDIES

JIMMA INSTITUTE OF TECHNOLOGY

FACULTY CIVIL AND ENVIRONMENTAL ENGINEERING

STRUCTURAL ENGINEERING STREAM

CONSTRUCTION OF UNIAXIAL INTERACTION DIAGRAM FOR SLENDER REINFORCED CONCRETE COLUMN USING NON LINEAR FE ANALYSIS SOFTWARE

A Thesis Submitted to Graduate Studies of Jimma University in Partial Fulfillment of the Requirements for the Degree of Master Science in Structural Engineering.

By: BEDASO AHMED

Main Advisor: Engr. Elmer C Agon (Asso. Prof.)

Co-Advisor: Engr. V.S. Ravi Kumar (Msc)

Nov, 2018

JIMMA, ETHIOPIA

JIMMA UNIVERSITY

JIMMA INSTITUTE OF TECHNOLOGY

POST GRADUATE PROGRAM

This is to certify that the thesis prepared by Bedaso Ahmed, entitled: ***"Construction of uniaxial interaction diagram for slender reinforced concrete column using nonlinear FE analysis software"*** and submitted in partial fulfillment of the requirements for the degree of masters of Science in Structural Engineering complies with the regulations of the university and meets the accepted standards with respect to the originality and quality.

Approved by the Examining Committee:

_____	_____	_____
Advisor	Signature	Date
_____	_____	_____
External Examiner	Signature	Date
_____	_____	_____
Internal Examiner	Signature	Date
_____	_____	_____
Chairman	Signature	Date

DECLARATION

I, the undersigned, declare that this thesis is my own work and all sources of material used for the thesis have been duly acknowledged. And it is also approved by my advisors.

Name: Bedaso Ahmed

Signature: _____ Date: _____

Place: Jimma University, Jimma Institute of Technology

Advisors

Main advisor: Engr. Elmer C Agon (Asso. Prof.)

Signature: _____ Date: _____

Co- advisor: Engr. V.S.Ravi Kumar (Msc)

Signature: _____ Date: _____

ACKNOWLEDGEMENT

Firstly, I would like to thanks Allah for making me strong and patient to finish the thesis. Next I like to express my gratitude to Jimma University Institute of Technology for supporting me financially. Then I like to express my especial thanks to my advisors Engr.Elmer C Agon and Engr.Ravi Kumar for their continuous advices and motivation. And also I would like to thanks Dr. Temesgen Wondimu for being volunteer in solving the problem which encounters me throughout the thesis work.

Finally, I would like to thank my family for supporting me in all manners throughout the thesis works.

Table of Contents

List of Tables

List of figures

Acronyms

ACI	American Concrete Institute
CAE	Complete Abaqus Environment
CFD	Computational Fluid Dynamics
EC-2	Euro code-2
Exp	Experimental
FE	Finite Element
FEA	Finite Element Analysis
NSM	Nominal Stiffness Method
RC	Reinforced Concrete
RCC	Reinforced Concrete Column
RP	Reference point
RRC1	Specimen number one of rectangular reinforced concrete column
RRC2	Specimen number two of rectangular reinforced concrete column
RRC3	Specimen number three of rectangular reinforced concrete column
RRC4	Specimen number four of rectangular reinforced concrete column
RRC5	Specimen number five of rectangular reinforced concrete column
RRC6	Specimen number six of rectangular reinforced concrete column
SLS	Serviceability Limit State
SRCC	Slender Reinforced Concrete Column
SRC1	Specimen number one of square reinforced concrete column
SRC2	Specimen number two of square reinforced concrete column
SRC3	Specimen number three of square reinforced concrete column
SRC4	Specimen number four of square reinforced concrete column
SRC5	Specimen number five of square reinforced concrete column
SRC6	Specimen number six of square reinforced concrete column
ULS	Ultimate Limit State

List of Notations

EI	Flexural rigidity of the column
L	Length of the column
n	Number of half sine in the deformed shape of the column
M_{ED}	Total design moment including second order moment
M_{oED}	First order moment
N_b	Buckling load based on nominal stiffness
N_{ED}	Design axial load
β	Factor which depends on distribution of 1st and 2nd order moments
E_{cd}	Design value of modulus of elasticity of concrete
I_c	Moment of inertia of the concrete cross-section
K_c	Factor for effect of cracking and creep.
K_s	Factor for contribution of reinforcement
E_s	Design value of modulus of elasticity of reinforcement
I_s	Second moment of area of reinforcement
ρ	Geometric reinforcement ratio
A_c	Area of concrete section
A_{st}	Total area of reinforcement
φ_{eff}	Effective creep ratio
K_1	Factor which depends on the concrete strength class
K_2	Factor which depends on axial force and slenderness
n’	Relative axial force
λ	Slenderness ratio
β_d	Factor to account for creep
M_2	Nominal second order moment
K_r	Correction factor depending on axial load
K_φ	Factor taking account of creep
ε_{c1}	Peak strain at peak stress
f_{cm}	Mean compressive strength at 28 days.

E_{cm} Secant modulus of elasticity of concrete

ε_c^{ch} Compressive crushing strain (inelastic strain)

l_{eq} Characteristic length of the element

f_{ck} Cylindrical compressive strength of concrete

G_{ch} Crushing energies of concrete

G_F Fracture energies of concrete

w_c Critical crack opening

ε_t^{ck} Tensile cracking strain (inelastic strain).

ε_{cm} Compressive strain of concrete at the extreme fiber

ε_{c2} Compressive strain of concrete at the peak stress

ε_{cu2} Maximum compressive strain of concrete

ABSTRACT

Slender reinforced concrete column may fail in material failure or instability failure. Instability failure is common problem which cannot be analyzed with first order analysis. So second order analysis is required to analyze instability failure of slender RC column. In second order analysis, the condition of equilibrium is satisfied in the deformed state of structure. As the deformation increases the material and load-displacement behaves in nonlinear manner. So nonlinear analysis is better for analysis of slender RC column.

In this study the capacity of uniaxial slender RC column which was illustrated by interaction diagram was done using nonlinear FE analysis software which is called ABAQUS 6.13. The key parameters which were studied in this thesis were eccentricity, slenderness ratio, amount of steel reinforcement and shape of the column. Concrete damage plasticity was used for modeling of material property of concrete and plastic for steel reinforcement bar and steel plate. Material nonlinearity, geometric nonlinearity, effect of cracking and tension stiffening effect were included in the modeling. Before modelling of specimen, validation was done by taking bench experiment. Validation results shows that the experimental load was 85.581% of FE result. Method used for validation was also used in modelling of all specimen. In modeling tie, embedded and coupling constraints were used. Dynamic explicit with bulk viscosity of 0.0015 was selected. Displacement control type with -0.004m/sec for loading and 0.02m mesh size for meshing was used. Using the job module, the analysis was run and the results were collected. Consequently, the axial load-moment interaction diagram was plotted. The diagrams reveal that as slenderness ratio increases, the balanced moment also increases but the corresponding axial load was decreased. But increasing amount of steel to the column increases the stability of the column and reduces the effect of slenderness ratio. For the same slenderness ratio increasing the amount of steel also increase the capacity of column. And also the capacity of square slender RC column is larger than rectangular slender RC column with equivalent cross-section. But the difference is reduced as slenderness ratio increased.

Finally, axial load-moment interaction diagram was prepared for all specimens using nominal stiffness method and comparison was done with the FEA results. It shows that the capacity of the column that results from FEA was greater than nominal stiffness method.

***Key words**: Uniaxial Interaction diagram, Eccentricity, Slenderness ratio, Amount of steel*

CHAPTER ONE

INTRODUCTION

1.1Background of the study

Column is a vertical member which is used to carry primarily compression loads. It is structural part of the building which receive the load from beam or directly from slab and transfer to the next consecutive lower floor column which it will be transfer finally to the foundation. Column may be subjected to axial with/without moments. Reinforced concrete column is one type of column in which its material is made from concrete and steel reinforcement bar. Reinforced concrete column may be short or slender (long) depending on slenderness ratio. According to Mac Gregor et al., short column is a column which can resist axial force and moment which is greater than or equal to axial and moment capacity of column cross section. But slender column is a column which its section resistance is reduced by second order deformation (Buckling) of the column. (Mac Gregor, et al. 1970)

Recently uses of slender reinforced concrete column are increasing to keep the aesthetic of the building and get the sufficient space inside of the building. (Kim,et al., 2006). So Analysis and design of this column is considering the second order deformation is necessary. Also Mac Gregor believes that the column should be designed to carry the axial load and moments that account the effect of second order deformation. (Mac Gregor, et al. 1970). Different country codes set on how to consider the second order effect in the design of slender reinforced concrete column. For example, Euro code-2 recommends Second Order Non-Linear analysis and Simplified methods such as second order analysis based on nominal stiffness method and based on estimation of the curvature. Other methods like Long column reduction factor method and Complementary moment design method also could be used. Except Second Order Nonlinear analysis the other all method uses approximate empirical equation to accounts for the second order deformation of the column. Although some of empirical equation does not account effect of cracking, the others account effect of cracking at location of maximum moment only. Cracking of the column reduces the flexural stiffness of the column. Since the crack will not form only at the location of the maximum moment, nonlinear analysis of slender column which accounts the effect cracking throughout the length is needed.

And also in the design of slender column using the above listed design method the tensile strength is ignored, though the member carries small tensile stress due to tension stiffening. So investigating the behavior of slender reinforced concrete column under nonlinear analysis including effect of cracking and tension stiffening effect is very important. Many researchers did different researches on this area like Kim and Kwak did a nonlinear behavior of slender Reinforced concrete column (Numerical formulation). (Kim, et al.,2006) Others also like Cleason and Gylltoft did experimental and FE analysis of slender concrete column subjected to eccentric loading (Cleason C. et al.,1998) and Rodrigues et al. on Failure behavior modeling of slender reinforced concrete column subjected to eccentric loading. (Rodrigues,et al., 2015). But none of them study construction of uniaxial interaction diagram for slender reinforced concrete column using nonlinear FE analysis.

In this paper construction of interaction diagram for uniaxial slender reinforced concrete column using nonlinear finite element software was studied. So the effect of cracking throughout length of column and effect tension stiffening on the uniaxial interaction diagram is also considered in this study.

1.2 Statement of the problem

Slender reinforced concrete column may fail in material failure or instability failure. Instability (Buckling) failure is common problem which cannot be analyzed with first order analysis. Because geometry, material properties (stress-strain relationship) and large deformations are nonlinear, nonlinear analysis should be performed to get better result. (Nessa Yosef, 2015). So exploring the behavior of the slender RC column under nonlinear analysis is important. Many researchers did research to determine the behavior of slender RC column. But still now the compression failure, tension failure and balanced failure load of slender RC column under nonlinear analysis which could be presented through interaction diagram is not done.

So in this research, elaboration of this behavior was determined through interaction diagram for uniaxial slender RC column.

1.3 Objective of the study

1.3.1 General objective

The general objective of this study was constructing uniaxial interaction diagram for slender reinforced concrete column using nonlinear finite element software.

1.3.2 Specific objective

- To model uniaxial slender reinforced concrete column which include both material and geometric nonlinearity, cracking effect and tension stiffening effect.
- To determine the capacity of uniaxial slender reinforced concrete column by considering the effect of slenderness ratio, geometrical steel ratio and shape of the column on capacity of the column which illustrated using interaction diagram.
- To validate the nonlinear FE analysis software result with experimental result.
- To prepare interaction diagram using nominal stiffness method by including material nonlinearity using Eurocode-2 and compare with FEA software result.

1.4 Significance of the study

This study determines the capacity of the uniaxial slender column which includes material and geometrical nonlinearity, cracking and tension stiffening effect. This enable us to recognize the change in capacity of the column due to the listed factors and motivate us to include it in design of Slender Reinforced Concrete Column.

1.5 Scope of the study

This research was limited to construct uniaxial interaction diagram using nonlinear FEA software by considering different slenderness ratio, geometrical steel ratio and shapes of RC column. While doing this research the knowledge FE software, FE analysis and design of reinforced concrete were used.

CHAPTER TWO

RELATED LITERATURE REVIEW

2.1 General Overview

Column is a structural member of the building in which it's chiefly intended to carry compressive load. Reinforced concrete column is one type of column in which its material is made of concrete and steel reinforcement bar. Column may be axial, uniaxial or biaxial depending on its loading. It may also short column or Slender (Long) column based on slenderness ratio of the column.

Mac Gregor believes that short column is a column which has axial and moment resistance greater or equal to cross sectional axial and moment resistance of the column and slender column is a column in which its cross sectional resistance is reduced by second order deformation of column. So column may be short or slender under a set of restraint or loading depending on their slenderness ratio. (Mac Gregor, et al. 1970). Now a day many buildings uses slender reinforced concrete column for their building in which aesthetic and also space inside the building is needed in addition to normal usage. (Kim, et al.,2006). So to enjoy the benefit of this slender reinforced concrete column knowing behavior, factors which affect strength, Analysis and design of slender reinforced concrete column is necessary.

2.2 Behavior of Slender RC Column

2.2.1 Buckling of Axially loaded Elastic Columns

Analysis and Design of Slender columns are different from short column due to buckling of the column when it is subjected to critical load. The column is buckle not due to applied load rather it is due to high slenderness ratio.

For illustration of elastic buckling three state of equilibrium are shown in the Figure 2-1. (J. MacGregor et al.,2005). If the ball in the Figure2-1(a) is displaced laterally and released, it will return to its original position. This is stable equilibrium. If the ball in the Figure2-1(c) is displaced laterally and released, it will roll of the hill. This is unstable equilibrium. The transition between stable and unstable equilibrium is neutral equilibrium, illustrated in Figure2-1(b). Here the ball will remain in the displaced position. Similar state of equilibrium

exists for axially loaded column in Figure 2-2(a). If the column is return to its original position when it is pushed laterally at mid height and released, it is in stable equilibrium; and soon.

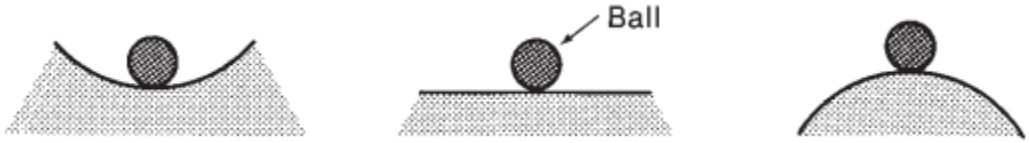

(a) Stable (b)Neutral (c) Unstable

Figure 2. 1: States of equilibrium (J. MacGregor et al.,2005)

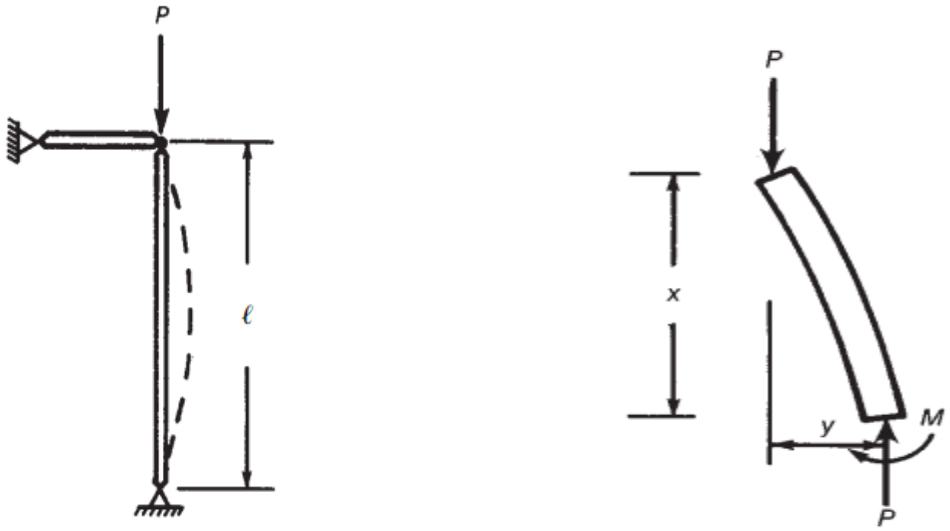

(a) Column (b) Free-body diagram

n=1 n=2 n=3

(c) Number of half sine wave

Figure 2. 2: Buckling of pin ended column (J. MacGregor, et al.,2005)

Differential equation for this equilibrium is

$$\frac{EId^2y}{dx^2}=-Py \qquad \text{Eqn.2-1, MacGregor et al. (12-3)}$$

In 1744, Leonhard Euler derive eqn.2-1 and its solution,

$$P_c=\frac{n^2\pi^2EI}{L^2} \qquad \text{Eqn.2-2, MacGregor et al. (12-4)}$$

Where

EI -flexure rigidity of the column

L-Length of the column

n=Number of half sine waves in the deformed shape of the column.

Cases with n=1,2 and 3 are illustrated in figure2-2(c). The lowest value of P_c will occur with n=1.This gives what is referred to as The Euler buckling load.

$$P_E=\frac{\pi^2EI}{L^2} \qquad \text{Eqn.2-3, MacGregor et al. (12-5)}$$

Such a column is shown in the figure 2-3(a). If this column were unable to move sideways at the mid height, as shown in the figure 2-3(b), it would buckle with n=2, and buckling load would be which is four times the critical load of the same column without mid height brace.

$$P_c=\frac{2^2\pi^2EI}{L^2}$$

Another way of looking at this involves the concept of the effective length of the column. The effective length is the length of pin ended column having the same buckling load. Thus the column in figure 2-3(c) has the same buckling load as that in figure2-3(b). The effective length of the column is L/2 in this case, where L/2 is the length of each of the half sine waves in the deflected shape of the column in figure2-3(b). The effective length, KL, is equal to L/n. The effective length factor K is 1/n.Eqn.2-2 is generally written as

$$P_c=\frac{\pi^2EI}{(KL)^2} \qquad \text{Eqn.2-4, MacGregor et al. (12-6)}$$

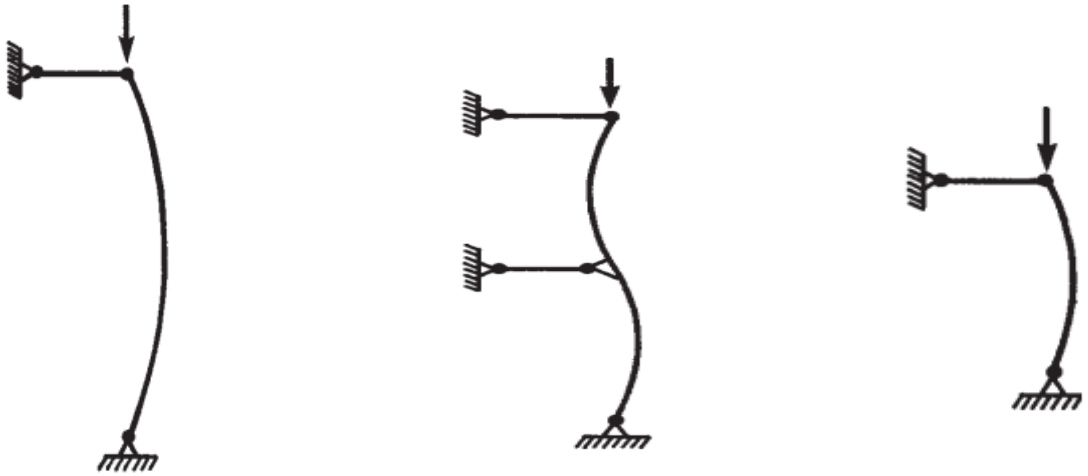

Figure 2. 3: Effective length of columns (J. MacGregor et al.,2005)

Though elastic column is too ideal, in equation 2-4, the critical load which is based on elastic buckling analysis is formulated for elastic column. But with many assumptions, steel column can behave elastically and hence their stability could be determined. So far, buckling curves have been produced for steel columns to assist steel column stability analysis such as European Buckling Curves. However, it is difficult to satisfy the conditions for elastic buckling analysis for RC column like steel column. Because Concrete is inelastic, section cracks affect its behavior, loading is eccentric, columns are not perfectly straight (Imperfection). Hence, Stability analysis of RC columns is carried out using second order theory. (Kabtamu Getachew, 2012).

2.2.2 Second Order Theory

In the first order theory, the equations of equilibrium are formulated on the un-deformed structure. In this theory, it assumes small deflection behaviors, and the resulting force and moments take no accounts additional effect due to deformation of the structure under load. This overestimates the capacity of the column. In Second order theory the condition of equilibrium is satisfied on the deformed structure. First order theory is sufficiently accurate for most structure like beam and slab. However, additional moment may not be negligible for columns due to presence of axial load especially for slender columns. (White, et al., 1991). So design of slender column should be done based on second order theory which accounts the effect of the deformation of the column.

2.2.3 Column Failure Mechanism

James Macgregor et al. illustrate the effect of slenderness on slender column using Figure2-4. The maximum moment in the column occurs at the section A-A, due to the combination of initial eccentricity e in the column and the deflection Δ at this point. Two types of failure can occur. First, the column may stable at deflection Δ_1 but the axial load P and the moment M at section A-A may exceed the strength of that cross section. This type of failure is Material failure and it is illustrated by column 1 Figure 2-4 (b). This type of failure is column failure which generally occurs in practical building columns which are braced against sway. Second as shown for column 2 in Figure 2-4(b),if the column is very slender it may reach a deflection Δ_2 due to the axial force P and the end moment Pe, such that the value of $\frac{\partial M}{\partial P}$ is zero or negative. This type of failure is known as a stability failure and may occur in slender columns in sway frames. (J. MacGregor ,et al., 1970). Stability failure also may occur in non-sway column.

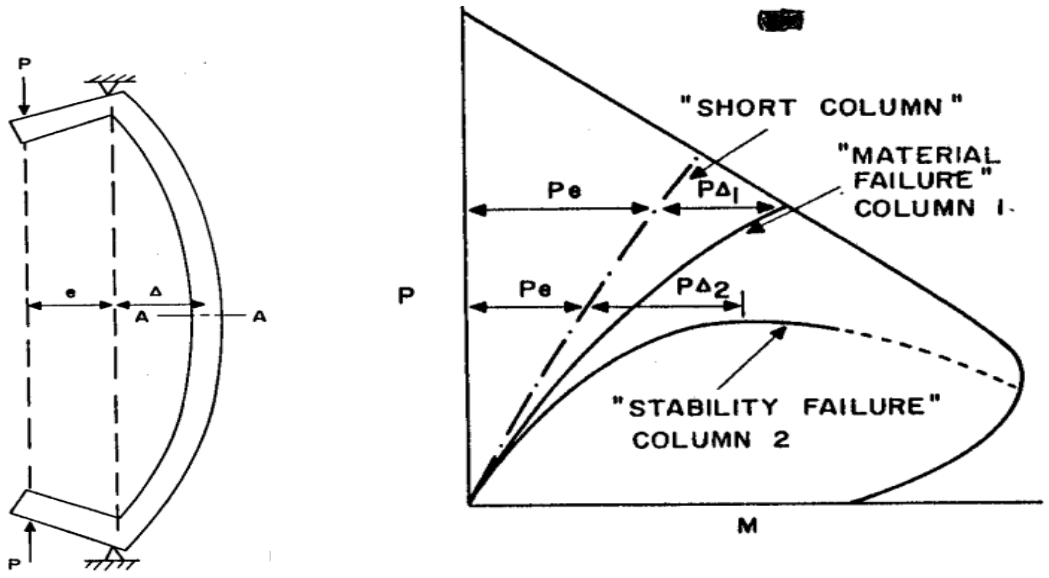

(a) (b)

Figure 2. 4: Load and moment in slender column

2.3 Major variables affecting the strength of slender column

Brom and Veist and, more recently, Pfrang and siess have presented comprehensive discussion of the effect of the number of variables on the strength of restrained and unrestrained columns. (James MacGregor, et al.,1970). These two studies shown that the three most significant variables affecting the strength and behavior of slender hinged column are: Slenderness ratio h/t, the end eccentricity e/t and the ratio of end eccentricity e_1/e_2. The effect of these variables is strongly interrelated, as illustrated in fig 2-5. MacGregor et al. presents this figures with three series load moment interaction curves for hinged column with various e_1/e_2 ratios. The interaction diagram is presented in terms of maximum load and moment that can be applied at the end of the columns with various slenderness ratios.

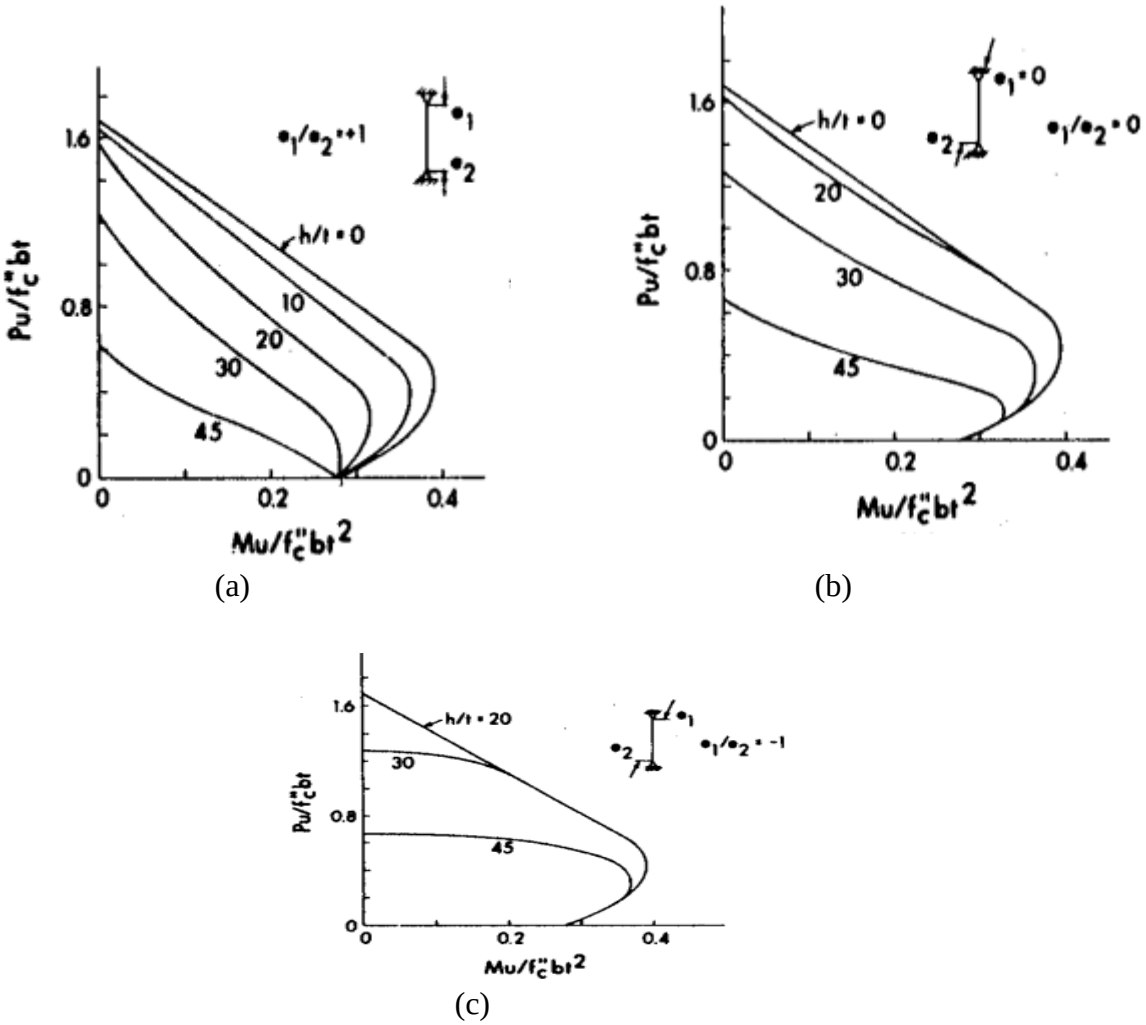

Figure 2. 5: Effect of deflected shape on interaction diagram for long hinged column.

A hinged column will be weakened if at any section the sum of the moment due to the end eccentricities or imperfection and the column deflection exceeds the maximum moment in the un-deflected column. In a column subjected to symmetrical single curvature the column deflection will always increase the column moments. Thus, in Figure2-5(a) the interaction diagram for all h/t values greater than zero fall inside the interaction diagram for cross-section (h/t=0).

In the case of double curvature, however, this will not always be true, since the maximum applied moment occurs at one or both ends of the column while the maximum deflection moments occur between the column ends. This is illustrated by the interaction diagram for h/t=30 in Figure 2-5(c). This column is weakened by the column deflection for small eccentricity where the sum of the deflection moments and applied moments lead to the maximum moments greater than the applied moments. For larger eccentricities, however, the maximum moments will always occur at the end of the column and as a result there is no weakening due to length. (James MacGregor, et al.,1970)

Broms and Viest showed that beyond the above discussed major variables the reinforcement ratio and strength of the concrete also have effect on the strength of slender column. They state that an increase in the proportion of the load carried by reinforcement led to the stable column but not for strength of the concrete. Thus, column with high concrete strength f_c' and/or low reinforcement percentage ρ tended to be most strongly affected. (James MacGregor, et al.,1970). This means as the concrete strength increases the column will be approach to unstable or to instability failure. But increment of steel will result into stable column.

Reduction of flexural stiffness, effect of sustained load and condition of restrained are another possible variable which affect the strength of slender RC column. Mirza also believe that the effective flexural stiffness of slender column is strongly affected by cracking along its length and inelastic action in the concrete and reinforcing steel. (Mirza,1990).

2.4 Analysis and Design of Slender RC Column

In the design of slender column, the analysis result which is used for the design should include the second order effect of the column. So the axial load and moment which is used for

design is based on the deformation of the column. James MacGregor et al. also share the same idea. (James MacGregor, et al.,1970). In order to incorporate the second order effect in the design of slender RC column different design method is used. Second order effect is included in the design of slender reinforced concrete column either using simplified method or Nonlinear analysis method. Simplified methods are Long column reduction factor method, Complementary moment design method (James MacGregor, et al.,1970), Design method based on nominal stiffness and design method based on estimation of curvature. But Nonlinear analysis method is performed using finite element software and it is accurate than others method. According to Euro code-2 and new EN EBCS-2 general method based on nonlinear second order analysis, design method based on nominal stiffness method and design method based on estimation of the curvature is recommended for the analysis of second order effect. (Eurocode-2,2002). ACI method also uses the moment magnifier method which is the same with nominal stiffness method but here constant value is used to account for effect of cracking. (ACI 318-89).

2.4.1 Nominal stiffness Method

In this method the second order effect is included by first determining the nominal flexural stiffness which accounts cracking and creep effect of the material. Material nonlinearity could be included depending the concrete uniaxial stress strain diagram. Then magnification factor will be calculated using the determined nominal stiffness and multiplied with first order moment if the factor is greater than one.

2.4.1.1 Nominal Stiffness method according to EC-2

In second order analysis based on stiffness, nominal values of flexural stiffness should be used, taking to account the effect of cracking, material nonlinearity and creep on the overall behavior. This also applies to the adjacent members involved in the analysis, e.g. beams, slabs and foundations.

$$M_{Ed}=M_{oEd}\left(1+\frac{\beta}{\frac{N_b}{N_{Ed}}-1}\right) \qquad \text{Eqn.2-5, EC-2 (5.28)}$$

But $N_b=\frac{\pi^2 EI}{L_e^2}$

The following model may use for nominal stiffness of slender compression member with an arbitrary cross-section:

$$EI=K_C E_{Cd} I_C+K_S E_S I_S \qquad \text{Eqn.2-6, EC-2 (5.21)}$$

Where:

M_{Ed}=The total design moment including second order moment.

M_{oEd}=is first order moment.

N_b=Buckling load based on nominal stiffness.

N_{Ed}=is the design value of axial load.

$\beta=\pi^2/C_o$=factor which depends on distribution of 1st and 2nd order moments.

E_{Cd}=design value of modulus of elasticity of concrete.

I_C =Moment of inertia of the concrete cross-section.

K_C =is a factor for effect of cracking and creep.

K_S =is a factor for contribution of reinforcement.

E_S=is the design value of modulus of elasticity of reinforcement.

I_S=Second moment of area of the reinforcement.

If $\rho\geq 0.002$ $K_S=1$ and $K_C=\frac{K_1 K_2}{1+\varphi_{eff}}$ Eqn.2-7, EC-2 (5.22)

Where, $K_1=\sqrt{\frac{f_{ck}}{20}}$ (Mpa) and $K_2=n\left(\frac{\lambda}{170}\right)\leq 0.2$ Eqn.2-8, EC-2 (5.23&5.24)

$$n=\frac{N_{Ed}}{A_c f_{cd}}$$

If λ is not defined K_2 may be taken as $K_2=n*0.3\leq 0.2$ Eqn.2-9, EC-2 (5.25)

If $\rho\geq 0.01$ $K_S=0$ and $K_C=\frac{0.3}{1+0.5\varphi_{eff}}$ Eqn.2-10, EC-2 (5.26)

Where: ρ=geometric reinforcement ratio,A_s/A_c

A_c=is the area of the concrete section

A_s=is the total area of the reinforcement

φ_{eff}=effective creep ratio.

K_1=is factor which depends on the concrete strength class

K_2=is a factor which depends on axial force and slenderness

n' =is relative axial force.

λ=Slenderness ratio

2.4.1.2 Nominal Stiffness method according to ACI

The ACI code also uses the same equation with EC-2 which is discussed above except in computation of nominal stiffness. In this code nominal stiffness is calculated using the following empirical equation.

$$EI=\frac{(0.2E_CI_C+E_SI_S)}{1+\beta_d} \qquad \text{Eqn.2-11, ACI318-89(10-14)}$$

Or

$$EI=\frac{(0.4E_CI_C)}{1+\beta_d} \qquad \text{Eqn.2-12, ACI318-89(10-15)}$$

β_d = is a factor to account for creep and it is ratio of factored dead load to factored total load.it is always taken positive.

2.4.2 Method based on nominal curvature

In this method the design moment is taken as:

$$M_{Ed}=M_{oEd}+M_2 \qquad \text{Eqn.2-13, EC-2 (5.31)}$$

Where: M_{oEd} is first order moment including the effect of imperfection.

M_2 is nominal second order moment.

$$M_2=N_{Ed}*e_2 \qquad \text{Eqn.2-14, EC-2 (5.33)}$$

$$e_2=\left(\frac{1}{r}\right)\left(\frac{l_o^2}{c}\right)$$

Where: e_2 is deflection, $\left(\frac{1}{r}\right)$ is the curvature, l_o is effective length and c is factor depending on the curvature distribution.

$$\left(\frac{1}{r}\right)=K_rK_\varphi\left(\frac{1}{r_o}\right) \qquad \text{Eqn.2-15, EC-2 (5.34)}$$

$$K_r=\frac{n_u-n}{n_u-n_{bal}}\leq 1 \qquad \text{Eqn.2-16, EC-2 (5.36)}$$

$$K_\varphi=1+\beta\varphi_{eff}\geq 1 \qquad \text{Eqn.2-17, EC-2 (5.37)}$$

$$\frac{1}{r_o}=\frac{\varepsilon_{yd}}{0.45d} \quad \text{where } \varepsilon_{yd}=\frac{f_{yd}}{E_s}$$

$$n_u=1+\omega \text{ where } \omega=\frac{A_sf_{yd}}{A_cf_{cd}}$$

Where: K_r is correction factor depending on axial load.

K_φ is factor taking account of creep.

d is effective depth and n is the relative axial force which is mentioned on nominal stiffness method.

Kabtamu Getachew prepare approximate uniaxial interaction diagram for slender reinforced concrete using the nominal curvature method which is provided on EBCS-2, 1995.But effect of creep and cracking was not included. This interaction diagram includes the second order moments and it is could be used as design aid for design of slender reinforced concrete column which is subjected to uniaxial loading. (Kabtamu Getachew, 2012).

2.4.3 Nonlinear analysis of slender column

In this method nonlinear analysis will be done to the column which includes geometric nonlinearity which is second order effect. Nonlinear method of analysis may be used for both ULS and SLS; provided that equilibrium and compatibility are satisfied and adequate

nonlinear behavior for material is assumed. Some of the studies which are performed on this area are presented below.

Kim et al. studied the nonlinear behavior of the slender column using finite element software. In these studies, the response of the column under nonlinear analysis Such as lateral deflection and the capacity of the uniaxial slender RC column under nonlinear analysis are studied. In this paper material nonlinearity, cracking and creep effect was considered. (Kim, et al., 2006). Kim et al. add another research which is continuous from the previous discussed one. The added studies are introduction of the design formula for slender RC column which is based on nonlinear analysis using regression. (Kim, et al.,2006). Rodrigues et al. also studied Failure behavior modeling of slender reinforced concrete columns subjected to eccentric load. In these studies, a numerical model to simulate the failure behavior of slender reinforced concrete column under eccentric compression load was studied and it emphasizes on the nature of the bond between steel and concrete during failure of slender column. (Rodrigues, et al.,2015). Nessa Yosef did second order FE analysis of biaxial loaded concrete members according to EC-2. In this study modeling of biaxial slender reinforced concrete column using Abaqus was done and analysis using Euro code was also prepared and compared with the software result. Behavior of the biaxial slender RC column using finite element software like lateral deflection and capacity of the column was also studied. (Nessa Yosef,2015).

2.5 Experimental Test on slender RC column

Kim et al. did experimental test to investigate the effect of concrete strength and longitudinal steel ratio on the buckling behavior of slender RC column. (Kim, et al.,1995) In this work a series of tests was carried out for 30 tied reinforced concrete column with 80mm square cross section and three slenderness ratios of 10, 60 and 100.Three different concrete of 25.5,63.5 and 86.2Mpa, and two different longitudinal steel ratios 1.98% and 3.95% were used. The boundary condition at the ends was both hinged and end eccentricities (24mm) were equal and the same sign. The experimental results revealed that the ultimate load for short high strength concrete column was significantly increased but not for slender column. The possibility of failure for slender column was increased with the increase of concrete strength. The increment of the ultimate load due to increase in longitudinal reinforcement for the short column was less than for the slender one, and heavier reinforcement for the slender column

led to a more stable column. This is illustrated in the research using different axial load-lateral deflection figure and interaction diagram. But here one axial load-lateral deflection for ρ=1.98% and λ=100 but for different strength of concrete that is for low, medium and high concrete strength and interaction diagram for ρ=1.98% and fc'=86.2Mpa is illustrated in figure2-6.

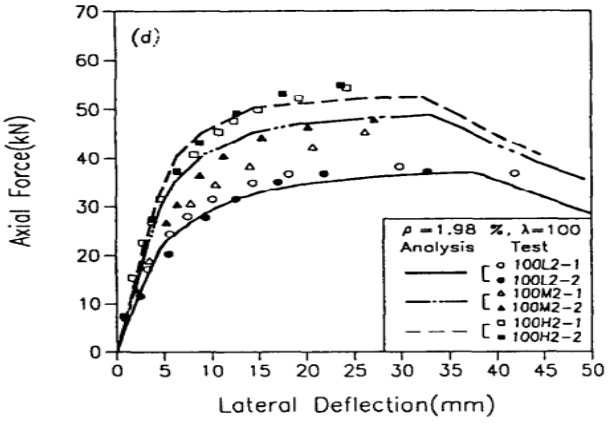

(a)Axial force-lateral deflection relations of the column

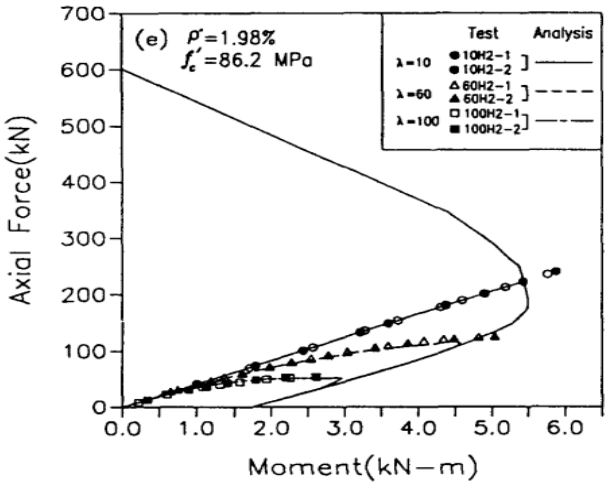

(b) Axial force-bending moment interaction diagram

Figure 2. 6: Axial Force-Lateral deflection curve and axial force-bending moment interaction diagram

Cleason et al. did experimental and modeling of high strength concrete columns subjected to eccentric loading. They take twelve full scale column with square section and tested under eccentric monotonic loadings. A parametric study was made to examine the difference in failure modes for different concrete strengths, length to width ratios and loading eccentricities. This paper finds that the higher compressive concrete strength was especially advantageous when the load eccentricity was small as it is illustrated in the fig 2-7. And also when the eccentricity was increased the strength of the high strength concrete columns decreased rapidly than that of the normal strength concrete columns. However, Claeson still believes that the high-strength concrete column still exhibited a greater load capacity than the normal strength concrete. (Cleason, et al., 1998).

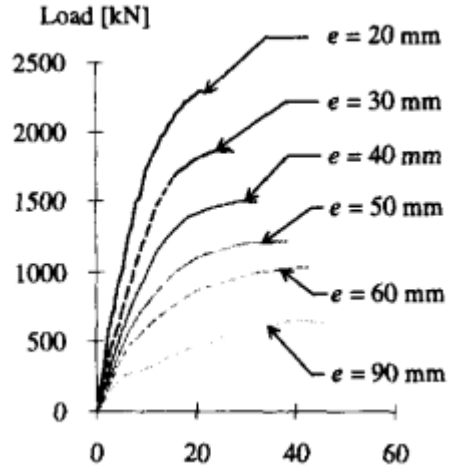

a) Load-mid height displacement for column with L 3m, 200*200 and fck=94.7Mpa.

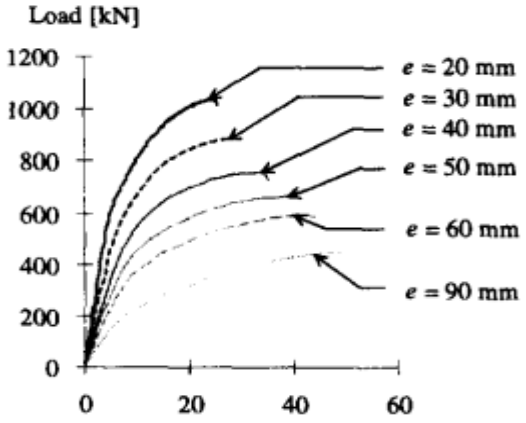

b) Load-mid height displacement for column with L 3m, 200*200 and fck=32.7Mpa

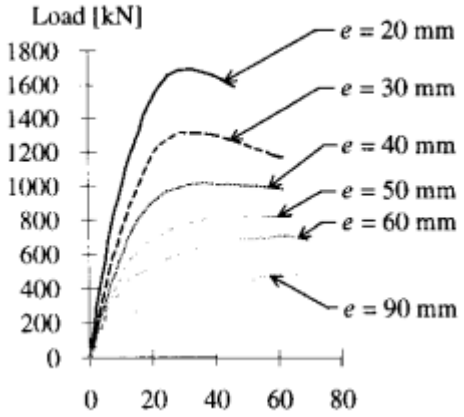

c) Load-mid height displacement for 4m, 200*200 and fck=94.7Mpa

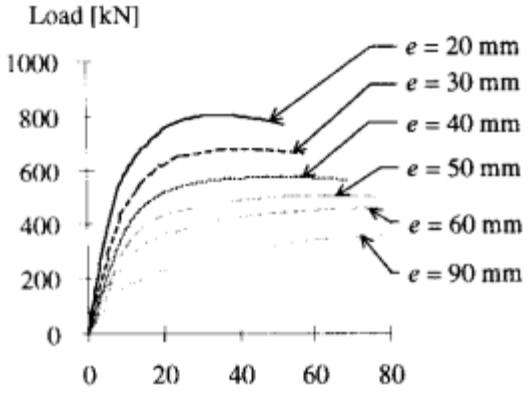

d) Load-mid height displacement for column with L=4m, 200*200 and fck=32.7Mp

Figure 2. 7: Load-mid height displacements for different column

Other experimental studies also carried out by Bazant et al on Failure of slender and stocky reinforced concrete column to investigate the size effect of the column on the failure of slender RC column. (Bazant, et al., 1994).

Generally, when the column is subjected to axial force and moment it may fail in compression, balanced or in tension depending on its loading. Points above the turning of the curve is the point which represents compression failure, points at the turning point of the interaction diagram is represent balanced failure and points below the turning point of the interaction diagram represent transition and tension failure. When the column is analyzed

using nonlinear analysis, the effect of cracking which reduce the flexural stiffness of the column and tension stiffening effect will be included. This both effects have influence on the capacity of the column which may change the compression failure, balanced failure and tension failure. This may also change the uniaxial interaction diagram of slender RC column. So as we try to discuss above on the research done on nonlinear analysis of the slender column section2.4.3, none of them did the interaction diagram of slender RC column using nonlinear FE analysis which considers the cracking and tension stiffening of the concrete.

In this thesis construction of uniaxial interaction diagram using nonlinear FE analysis was done. The effect of Cracking, Tension stiffening, material nonlinearity and geometric nonlinearity (second order effect) was included.

CHAPTER THREE

RESEARCH METHODOLOGY

3.1 General

Starting from the idea and proceed to decide the research area which is slender RC column, research topic was fixed first. Then literature review was done before deciding on the title and the problem was identified through reviewing the related literature. Consequently, the title was decided and planning was done to solve the identified problem. Before starting modelling, software training was held for one and half month to determine the way of modelling, the capability of the software and related theories which incorporated in the software. Based on the amount of the work and time, the number of variables was decided. Specimen for reinforced concrete column was prepared based on the variable which was studied in this thesis.

3.2 Research Design

The research was theoretical research which means modelling of the column using FEA software. In this thesis experimental work was not done.

3.3 Study Variables

3.3.1 Dependent study variables

Dependent study variable was Interaction diagram which is set of Axial load capacity and Moment capacity.

3.3.2 Independent Variables

Independent study variables were diameter of reinforcement bar, number of reinforcement bar, eccentricity, geometrical steel ratio, slenderness ratio and shape of the column.

3.4 Specimen selection

The specimen was selected based on the above variable and also the benchmark experiment is considered. The key parametric study was slenderness ratio, geometrical steel ratio, Shape of

the column, axial load eccentricity. To draw the interaction diagram for one specimen around fifteen points which is combination of axial load and moment was considered. So based on the above discussion the following column specimen was selected and modeled.

The material property was prepared while modelling for validation. So concrete grade and steel grade was taken from benchmark experiment.

Table 3. 1: Column specimen

No.	Specimen	C	fyk	b	h	L	λ	#Bar	dia	ρ
1	SRC1	43	636	200	200	3500	60.62	4	12	0.0122267
2	SRC2	43	636	200	200	4650	80.54	4	12	0.0122267
3	SRC3	43	636	200	200	5800	100.46	4	12	0.0122267
4	SRC4	43	636	200	200	3500	60.62	4	14	0.016642
5	SRC5	43	636	200	200	4650	80.54	4	14	0.016642
6	SRC6	43	636	200	200	5800	100.46	4	14	0.016642
7	RRC1	43	636	19	210	3330	60.7	4	12	0.0122102
8	RRC2	43	636	190	210	4420	80.58	4	12	0.0122102
9	RRC3	43	636	190	210	5510	100.46	4	12	0.0122102
10	RRC4	43	636	190	210	3330	60.7	4	14	0.0166195
11	RRC5	43	636	190	210	4420	80.58	4	14	0.0166195
12	RRC6	43	636	190	210	5510	100.46	4	14	0.0166195

3.5 Nonlinear Finite Element Software

In this research Nonlinear Finite element analysis software which is called ABAQUS 6.13 is used. Abaqus finite element system includes Abaqus CAE, Abaqus viewer, Abaqus /standard, Abaqus/ explicit and Abaqus/CFD. Each of them is clearly described below.

- **Abaqus/CAE:** is a complete Abaqus environment that provides a simple, consistent interface for creating, submitting and evaluation results from Abaqus analysis products. Abaqus/CAE is divided into modules, where each module defines a logical aspect of the modeling process. As you move from module to module, you build the model from which Abaqus/CAE generates an input file that you submit to the abaqus analysis product. The analysis product performs the analysis, sends information to Abaqus/CAE to allow you to monitor the progress of the job and generates an output

database. Finally, using the visualization module of Abaqus/CAE to read the output database and view the results of analysis. (Abaqus/CAE userguides,2013).

- **Abaqus/Viewer:** provides graphical display of Abaqus finite element models and results. Abaqus/Viewer is incorporated into Abaqus/CAE as Visualization module.
- **Abaqus/Standard:** is general purpose analysis product. It can solve a wide range of linear and nonlinear problems involving the static, dynamic, thermal, electrical and electromagnetic response of components.
- **Abaqus/Explicit**: It is the other type of analysis product which provides nonlinear, transient, dynamic analysis of solids and structures using explicit time integration. Its powerful contact capabilities, reliability and computational efficiency on large models also make it highly effective for quasi-static applications involving discontinuous nonlinear behavior.
- **Abaqus/CFD:** This product is a computational fluid dynamics program with extensive support for preprocessing, simulation and post processing in Abaqus/CAE.it provides scalable parallel CFD simulation capabilities to address a number of nonlinear coupled fluid-thermal and fluid structural problems. (Abaqus release note,2013).

So, uniaxial slender reinforced concrete column is modeled and submitted to analysis product using Abaqus/ CAE.

Geometrically nonlinear static problems sometimes involve buckling or collapse behavior, where the load displacement response shows a negative stiffness and structure must release strain energy to remain in equilibrium. Several approaches are possible for modeling such behavior. One is to treat the buckling response dynamically. Another approach would be to use dashpots to stabilize the structure during the static analysis (Abaqus Analysis 2, 2013). Since slender reinforced concrete column involve buckling or collapse behavior, Abaqus /explicit is selected for the analysis to analyses the buckling response dynamically.

3.6 Modeling of Slender RC column.

Before modeling of the specimen the validation works which is described in chapter four is done using method described in this chapter. The modeling procedure is described below and illustrated in Fig3.1.

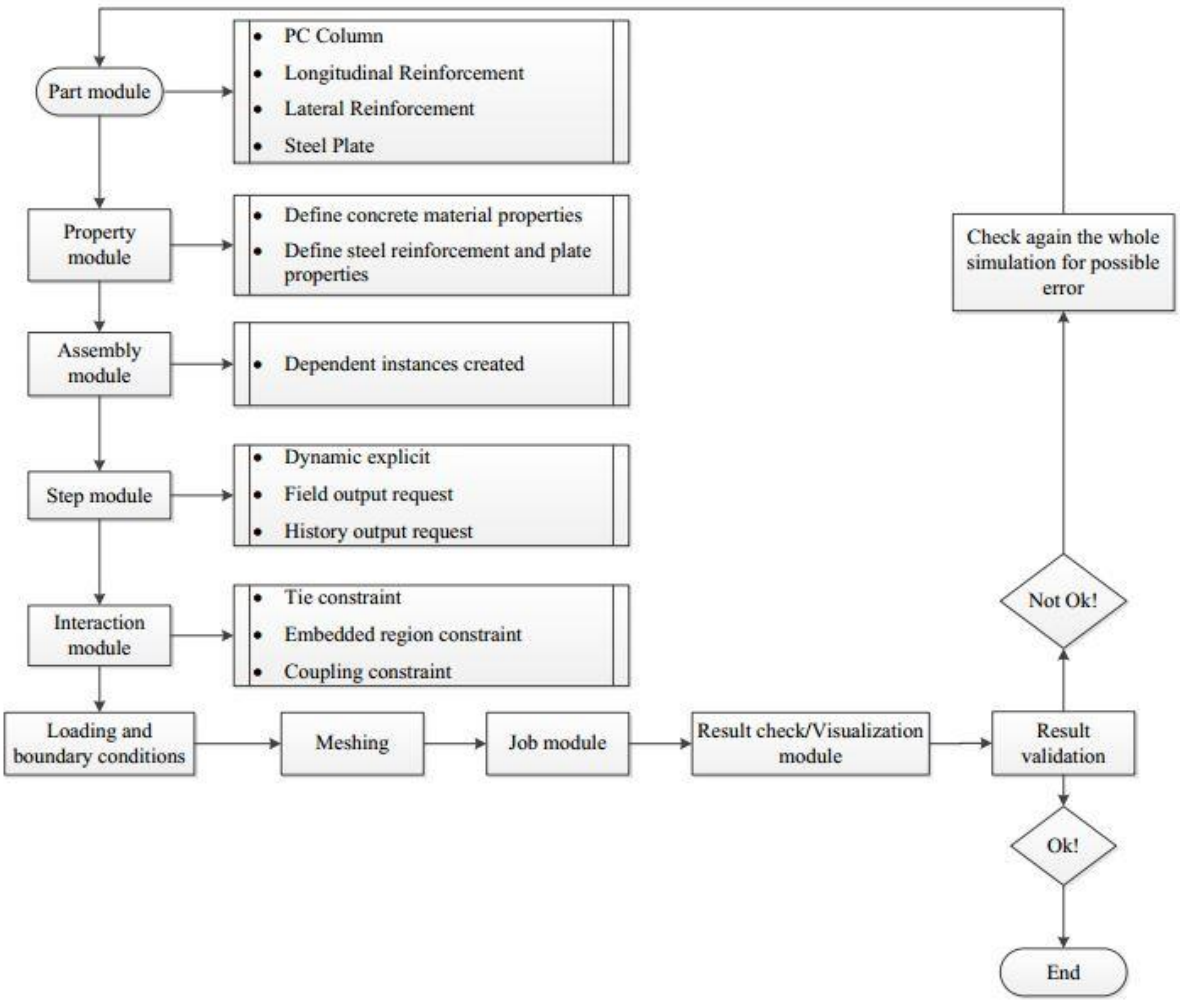

Figure 3. 1: Chart shows the procedure of modeling.

3.6.1 Geometry

a) Plain concrete column

Square and rectangular column was modeled using 3D, deformable and extrusion method. It is shown in Fig 3.2. In order to keep the compatibility between steel plate and RC column the partition was created. This also enables us to refine the mesh and get better result.

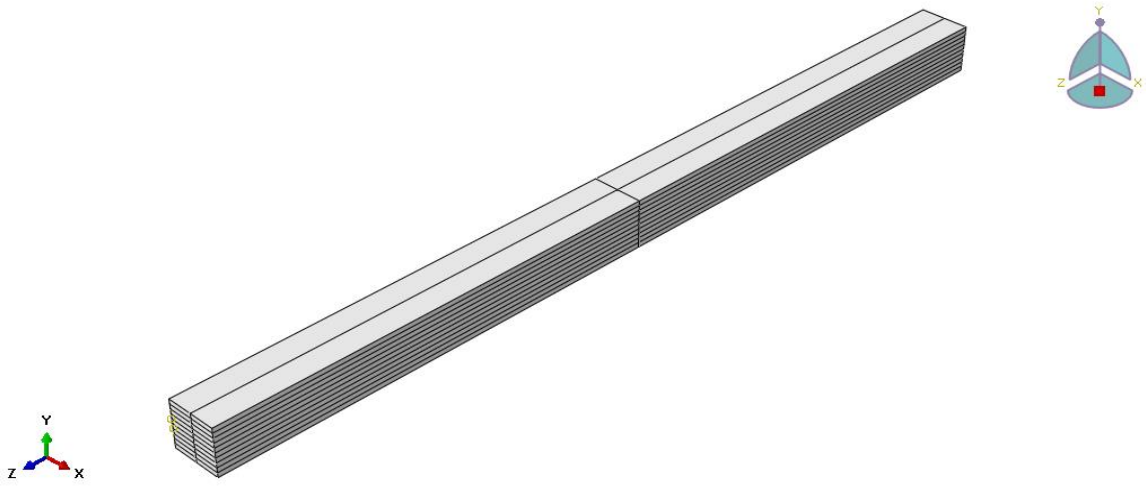

Figure 3. 2: 3D plain concrete part for SRC1

b) Longitudinal Reinforcement

It was modeled using 3D, deformable and wire method.

c) Lateral reinforcement

It was modeled using 3D, deformable and wire method.

d)Steel Plate

Steel Plate was used at the top end and bottom end of the column. It was modeled using 3D, deformable and extrusion method. Thickness of 20mm was used and size of plate is 600mm by 600mm for square and 590 by 600mm for rectangular columns were used.

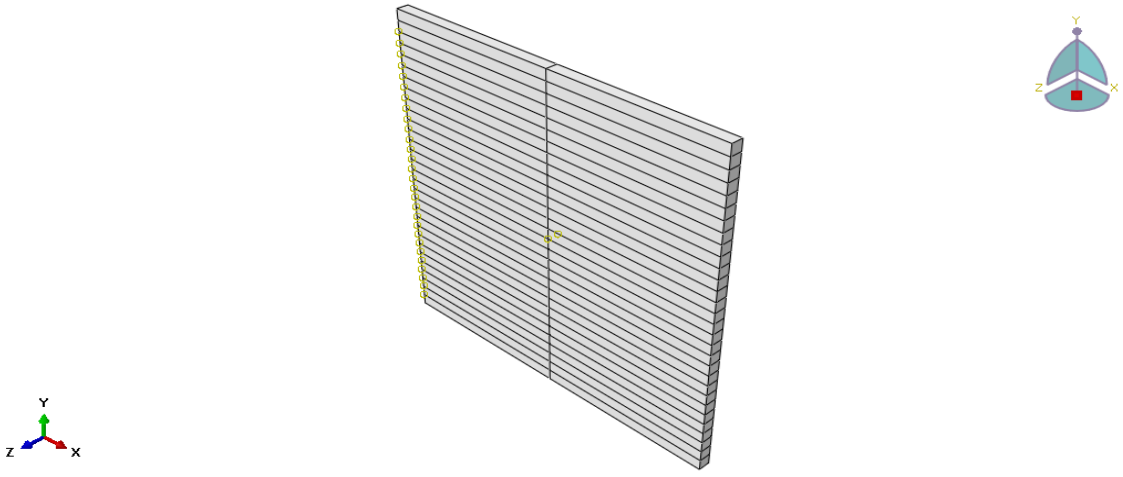

Figure 3. 3: Steel plate for end of the column.

3.6.2 Material property

Experimental data of Claeson, et al was used for both concrete and steel. (Claeson C., et al., 1998).

a) Concrete

Three different constitutive models are offered in Abaqus for the analysis of concrete at low confining pressures. These constitutive models are:

- Smeared crack concrete model
- Brittle cracking model
- Concrete damaged plasticity model

From the above mentioned model, smeared crack model is available only in Abaqus/Standard and Brittle cracking model is available only in Abaqus/Explicit. But concrete damaged plasticity is available in both Abaqus/Standard and Abaqus/Explicit. Each model is designed to provide a general capability for modeling plain and reinforced concrete in all types of structures. Brittle cracking model assumes that compressive behavior is always linear elastic. (Abaqus Analysis 3,2013). Since Abaqus/Explicit was selected and compressive behavior is nonlinear concrete damage plasticity model was chosen.

- **Concrete damage plasticity model**

Alfarah et al. state that concrete exhibit nonlinear stress-strain response mainly because of micro-cracking. Cracks are oriented as the stress field and generate the failure modes. In tension, failure localized in a narrow band; stress-strain behavior is characterized by sudden softening accompanied with reduction in the unloading stiffness. In compression, failure begins usually in the outside and is more complex, involving volumetric expansion, strain localization, crushing, and inclined slipping and spalling; stress-strain behavior involves ductile hardening followed by softening and reduction in the unloading stiffness. (Alfarah B., et al., 2017). Concrete damage plasticity model have shown good performance in capturing concrete behavior which is mentioned above in tests on full-scale structures. (Nguyen G., et al., 2008). This model is particularly well suited for reproducing failure modes that are based on tensile cracking and compression crushing. (Alfarah B., et al., 2017).

When the concrete specimen is unloaded from any point on the strain softening branch of the stress-strain curves, the unloading response is observed to be weakened: the elastic stiffness of the material appears to be damaged (or degraded). The degradation of the elastic stiffness is significantly different between tension and compression tests. In either case, the effect is more pronounced as the plastic strain increases. The degraded response of concrete is characterized by two independent uniaxial damage variables d_t and d_c which are assumed to be functions of the plastic strain, temperature and field variables. The uniaxial degradation variables are increasing functions of the equivalent plastic strains. They can take values ranging from zero, for the undamaged material to one for the fully damaged material. If E_o is the initial (undamaged) elastic stiffness of the material, the stress-strain relations under uniaxial tension and compression loading are, respectively: (Abaqus Theory,2013).

$$\sigma_c=(1-d_c)E_o(\varepsilon_c-\varepsilon_c^{pl}) \qquad \text{Eqn.3-1}$$

$$\sigma_t=(1-d_t)E_o(\varepsilon_t-\varepsilon_t^{pl}) \qquad \text{Eqn.3-2}$$

The parameters which were used in this model that was input for the software was discussed below:

For dilation angle, eccentricity, ratio of compressive biaxial to compressive uniaxial ($\frac{\sigma_{bo}}{\sigma_{co}}$) , Constant K_c and viscosity the default value was used. The default values are listed below.

Table 3. 2: Property of Concrete

Density	2400Kg/m^3
Modulus of elasticity	33.5937 Mpa(Eqn.3-3)
Poisson ratio	0.2 (EC-2,2004)
Dilation angle	36 (default)
Eccentricity	0.1 (default)
f_{bo}/f_{co}	1.16 (default)
Constant,Kc	0.6667 (default)
Viscosity	0 (default)

i) Uniaxial Compressive strength of concrete

Cubic compressive strength of the concrete which was used in this thesis is 43Mpa.Uniaxial compressive stress-strain diagram which is provided on Euro code for nonlinear analysis was used. It was drawn from Equation which is provided on EC-2, Sec3.1.5 and also discussed below:

$$\frac{\sigma_c}{f_{cm}} = \frac{k\mu - \mu^2}{1+(k-2)\mu} \qquad \text{Eqn.3-3,EC-2,(3.14)}$$

Where:

$$\mu = \frac{\varepsilon_c}{\varepsilon_{c1}}$$

$$k = \frac{1.05E_{cm}|\varepsilon_{c1}|}{f_{cm}}$$

$$0<|\varepsilon_c|<|\varepsilon_{cu1}|$$

ε_{c1} is peak strain at peak stress

f_{cm} is the mean compressive strength at 28 days.

E_{cm} is secant modulus of elasticity of concrete.

Equation which is provided in EC-2, Table 3.1 was used for, ε_{c1}, E_{cm}, f_{cm} and ε_{cu1} and also listed below.

$$f_{cm} = f_{ck} + 8 \ \text{(Mpa)} \qquad \text{Eqn.3-4}$$

$$E_{cm} = 22\left[\frac{f_{cm}}{10}\right]^{0.3} \quad \text{where } f_{cm}\text{(Mpa)} \qquad \text{Eqn.3-5}$$

$$\varepsilon_{c1}(\%o) = 0.7f_{cm}^{0.31} < 2.8 \qquad \text{Eqn.3-6}$$

$$\varepsilon_{cu1}(\%o) = 3.5$$

So, $0<|\varepsilon_c|<3.5$ was considered. Using the above mentioned compressive cylindrical strength each point of the curve was determined and plotted as follows: But the tabulated result is presented in appendix A, Table A.1.

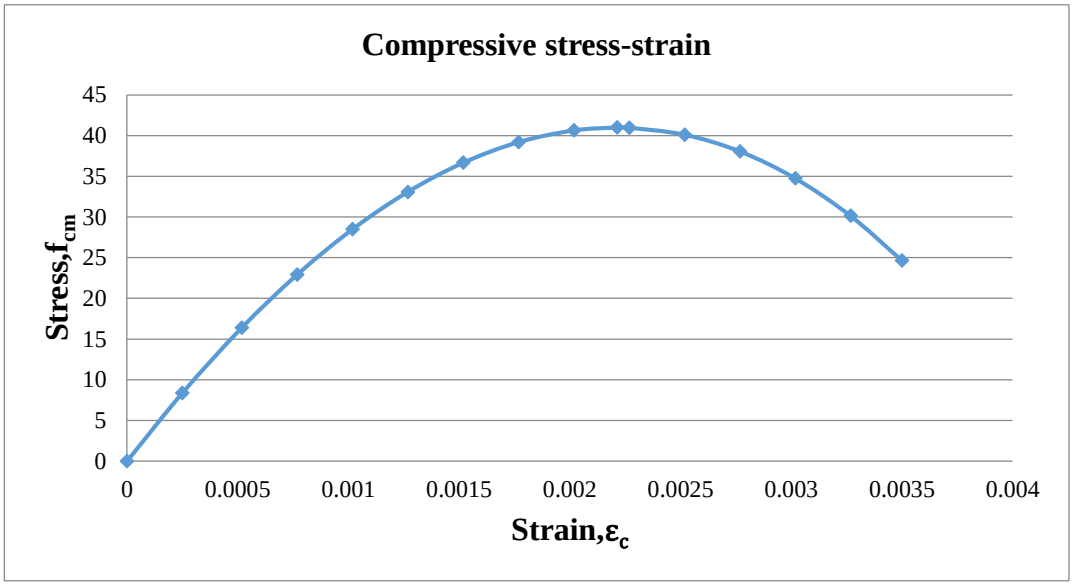

Figure 3. 4: Compressive stress-strain diagram of concrete

But the input which was used for Abaqus is Compressive stress-crushing strain. Crushing strain was calculated by deducting elastic strain from total strain. The diagram is plotted below but the table is presented in appendix A.

$$\varepsilon_c^{ch}=\varepsilon_{tot} - \frac{\sigma_c}{E_c} \qquad \text{Eqn.3-7}$$

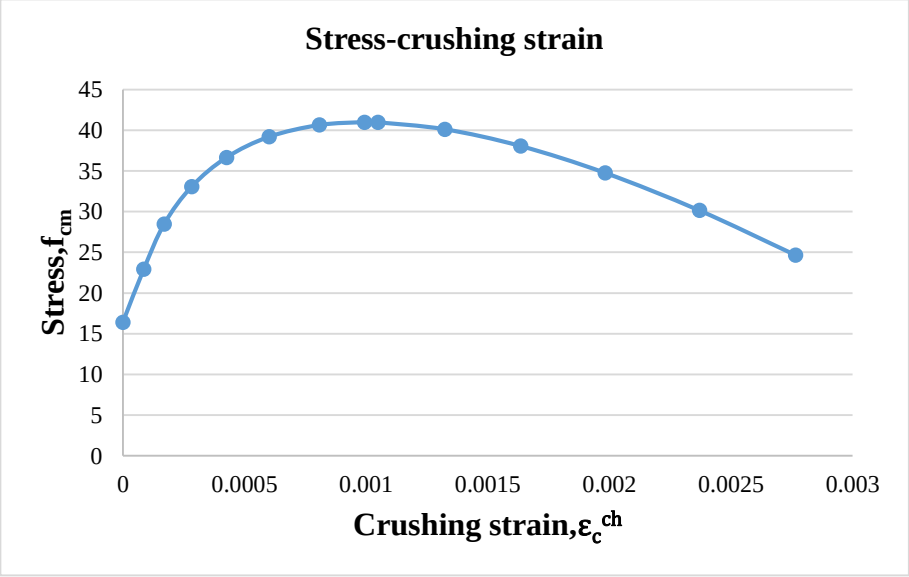

Figure 3. 5: Compressive stress-crushing strain diagram of concrete.

ii) Compressive damage variables

The damage variables were prepared based on Alfarah B., et al. proposed methodology and equation. This equation is described as follows: (Alfarah B.,et al.,2017).

$$d_c=1-\frac{1}{2+a_c}\left[2(1+a_c)\exp\left(-b_c\varepsilon_c^{ch}\right)-a_c\exp\left(-2b_c\varepsilon_c^{ch}\right)\right] \qquad \text{Eqn.3-8(19)}$$

Where: ε_c^{ch} is compressive crushing strain (inelastic strain).

$$a_c=7.873,\ b_c=\frac{1.97(f_{ck}+8)l_{eq}}{G_{ch}} \qquad \text{Eqn.3-9(34)}$$

Where: l_{eq} is the characteristic length of the element.

f_{ck} is cylindrical compressive strength of concrete.

G_{ch} is crushing energies, G_F is fracture energies.

$$G_{ch}=\left(\frac{f_{cm}}{f_{tm}}\right)^2 G_F \qquad \text{Eqn.3-10(32)}$$

$$G_F(\text{N/mm})=0.073f_{cm}^{0.18}, \qquad f_{cm}(\text{Mpa}) \qquad \text{Eqn.3-11(31)}$$

Using these equation damage variables were computed and tabulated. Compressive damage variable-crushing strain is illustrated below but the table is presented in appendix A.

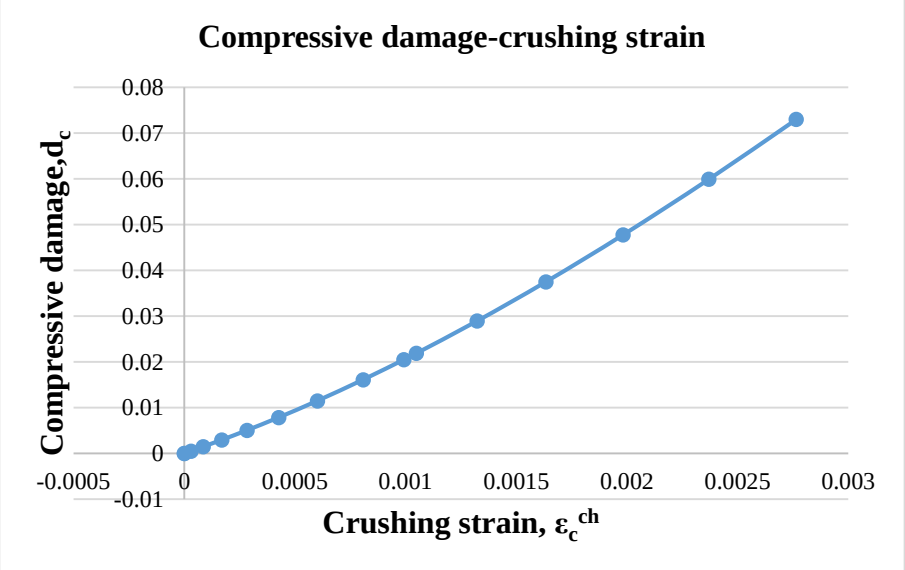

Figure 3. 6: Compressive damage-crushing strain diagram of concrete.

iii) Tensile strength of concrete

For tensile behavior, the equation which is provided on Hordijk was used (Hordijk, 1992).The ratio of tensile stress $\sigma_t(w)$(for crack width w) and maximum tensile strength f_{tm} is given as follows:

$$\frac{\sigma_t(w)}{f_{tm}} = \left[1+\left(c_1\left(\frac{w}{w_c}\right)\right)^3\right]e^{-c_2\left(\frac{w}{w_c}\right)} - \left(\frac{w}{w_c}\right)\left(1+c_1^3\right)e^{-c_2} \qquad \text{Eqn.3-12(29)}$$

In equation 3-8,c_1=3,c_2=6.93(Hordijk,1992) and w_c is the critical crack opening. The equation 3-12 shows that $\sigma_t(0)=f_{tm}$ and $\sigma_t(w_c)=0$.Therefore,w_c can be considered as the fracture crack opening.(Alfarah,2017).

$$w_c = \frac{5.14G_F}{f_{tm}} \qquad \text{Eqn.3-13(30)}$$

$$f_{tm} = 0.3016f_{ck}^{\frac{2}{3}} \qquad \text{Eqn.3-14}$$

In this proposed method the actual crack spacing was not studied but single crack per element has been assumed. Alfarah et al. agree that the assumption is suitable for global-purpose simulation. After this assumption, in the descending segment of the tensile stress-strain curve, the strain can be obtained in terms of the crack opening from the following kinematic relation. (Alfarah et al.,2017):

$$\varepsilon_t = \varepsilon_{tm} + \frac{w}{l_{eq}} \qquad \text{Eqn.3-15(33)}$$

Based on the above discussed method tensile stress-strain of concrete was computed and tabulated and plotted in appendix A. But stress-cracking strain which was used as input data for the software is plotted in Fig 3.5. Cracking strain was calculated by deducting elastic strain from total strain.

iii) Tensile damage variables

As it is discussed in compressive damage variables the same method was employed also for tensile damage variables and it is described as follows:

$$d_t=1-\frac{1}{2+a_t}\left[2(1+a_t)\exp\left(-b_t\varepsilon_t^{ck}\right)-a_t\exp\left(-2b_t\varepsilon_t^{ck}\right)\right] \qquad \text{Eqn.3-16(20)}$$

Where: ε_t^{ck} is tensile cracking strain (inelastic strain).

$$a_t=1,\ b_t=\frac{0.453(f_{ck})^{\frac{2}{3}}l_{eq}}{G_F} \qquad \text{Eqn.3-17(34)}$$

Using equation 3-16,tensile damage variables were computed and tabulated.Tensile damage variables-cracking strain is plotted in Fig3.6.But the table is presented in appendix A.

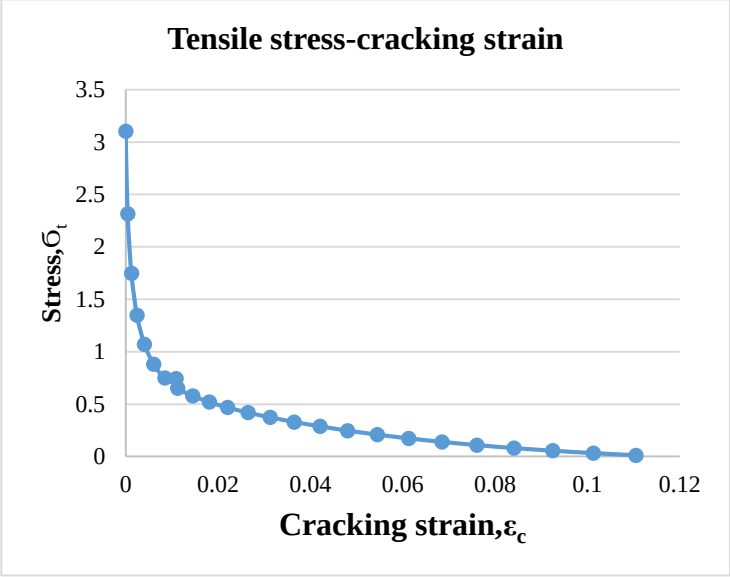

Figure 3. 7: Tensile stress-cracking strain diagram of concrete.

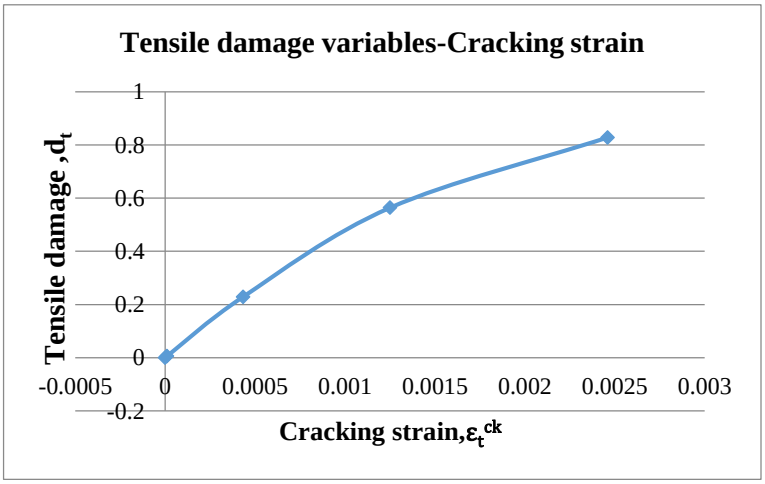

Figure 3. 8: Tensile damage variables-cracking strain diagram of concrete.

b) Steel

For all of the following steel, density of 7850Kg/m^3 and Poisson ratio of 0.3 were used.

i) Reinforcement bar

As it is mentioned at the beginning of section 3.6.2 data for steel was taken from claeson et al study. Deformed bars of Swedish type Ks40S were used as the lateral reinforcement and Ks60 for the longitudinal reinforcement. The mechanical properties of steel reinforcement which is provided by claeson et al. are presented in the following table3.3. (Claeson C.,et al.,1998).

Table 3. 3: Mechanical properties of steel reinforcement

Specimen	f_y(Mpa)	f_u(Mpa)	ε_{sh}(%)	ε_u(%)	E_s(Gpa)
Φ16 Ks60	636	721	2.2	10	207
Φ8 Ks40S	466	620	4	12	221

But it is difficult to get the stress-strain part which is after strain hardening from given data. So equation was developed from the given data and compare with provided graph on claeson et al. This equation written as follows:

For longitudinal Reinforcement bar

$$\sigma_s=-13971.1\varepsilon^2+2794.214\varepsilon+581.2893,\ 0.022\leq\varepsilon\leq0.1 \qquad \text{Eqn.3-18}$$

For lateral reinforcement bar

$$\sigma_s=-24062.5\varepsilon^2+5775\varepsilon+273.5,\ 0.04\leq\varepsilon\leq0.12 \qquad \text{Eqn.3-19}$$

So using this equation stress and strain was computed and tabulated in Appendix A. And stress-strain diagram also provided in appendix A. But true stress-logarithmic plastic strain was used as input data for the software which was computed based on true stress and logarithmic strain equation. The equation which was used to compute true stress and logarithmic plastic strain from nominal stress and nominal strain is presented as follows (Abaqus Analysis-3,2013):

$$\sigma_{true}=\sigma_{nom}(1+\varepsilon_{nom}) \qquad \text{Eqn.3-20}$$

$$\varepsilon_{ln}^{pl}=\ln(1+\varepsilon_{nom})-\frac{\sigma_{true}}{E} \qquad \text{Eqn.3-21}$$

Using nominal stress and strain, true stress and logarithmic plastic strain was computed and tabulated in appendix A but the diagram is plotted below.

For Longitudinal reinforcement

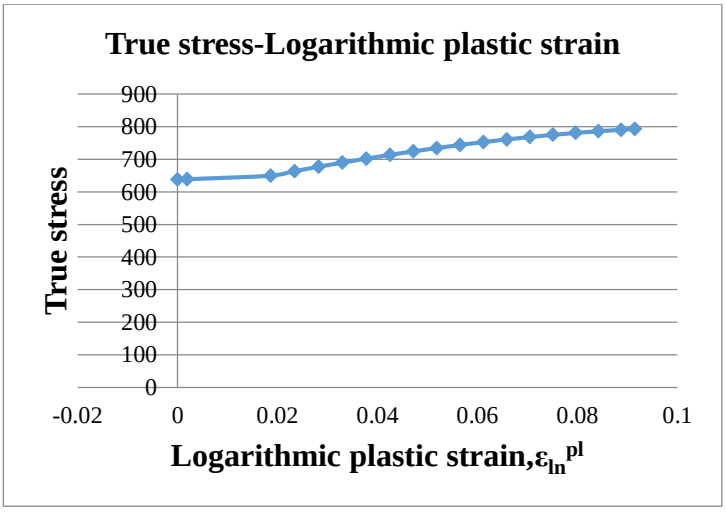

Figure3. 9: True stress-plastic strain of longitudinal steel reinforcement.

For Lateral reinforcement

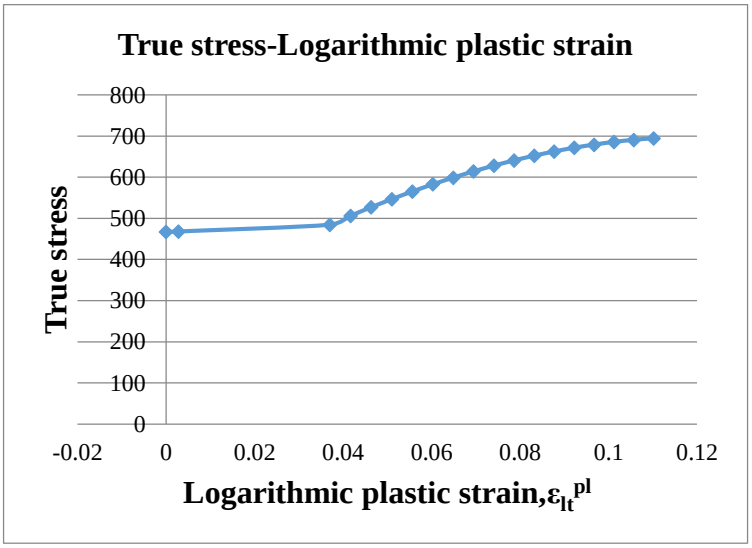

Figure3. 10: True stress-plastic strain of lateral steel reinforcement.

ii) Steel plate

For steel plate the property of longitudinal reinforcement was used.

After material properties were created, profile and section for each part were prepared and assign to their corresponding parts.

3.6.3 Part assembly and their Interaction

Instances were created for each part which was created at beginning of modeling and all instances were assembled to their relative position. Dependent instance was used. Spacing for lateral reinforcement that is used in the modeling was 130mm which was used in validation.

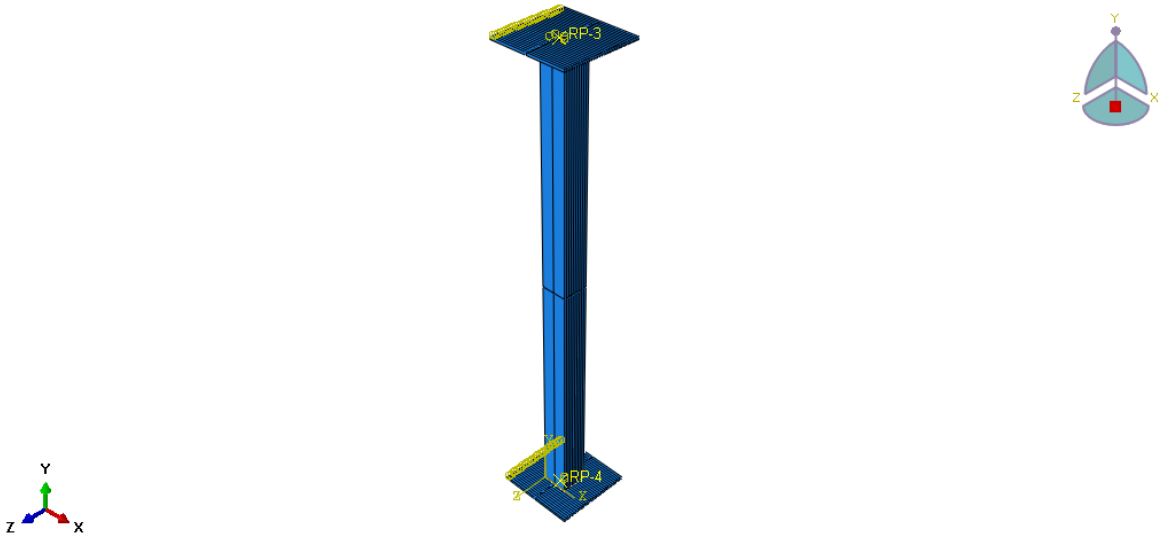

Figure3. 11: Assembled slender reinforced concrete column using Abaqus for SRC1

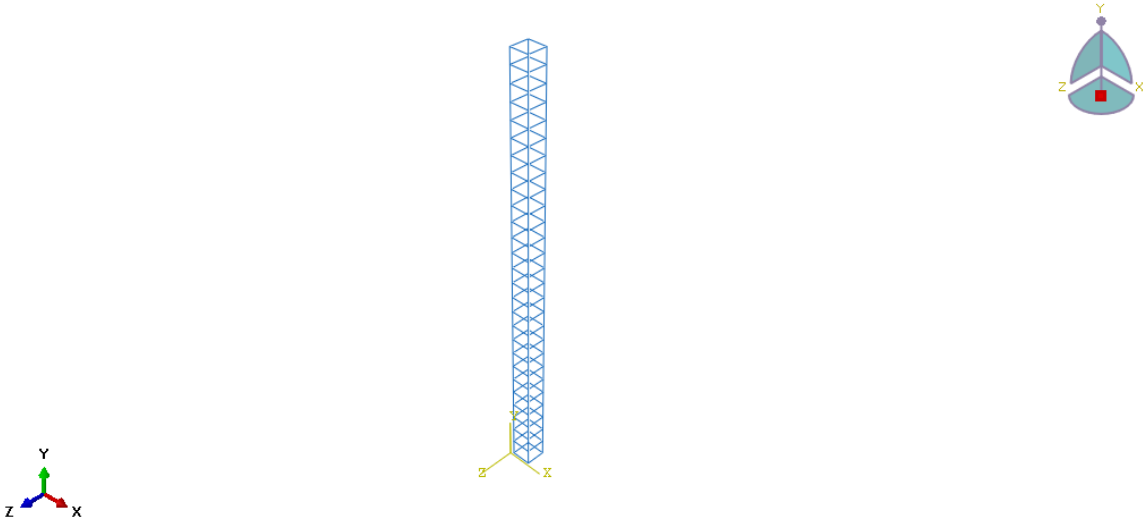

Figure3. 12: Assembled longitudinal and lateral reinforcement using Abaqus for SRC1

For reinforcement bar embedded region constraint was used by considering reinforcement as embedded part and concrete as a host. This type of constraint was used to create the strong bond between reinforcement and concrete. But for the region between column end and steel plate, tie constraint was used by taking column surface as a master and plate surface as slave. This constraint enables both column and steel plate to act as one body. The final constraint which was used in the modeling was coupling constraint. Coupling was done between plate surface and reference point which is act as control points. Control point was changed as eccentricity was changing. This constraint makes the steel plate to act as discrete rigid and prevent deformation due to applied loading on its surface.

3.6.4 Analysis step

In addition to initial step only one step was created. In the created step dynamic explicit method was selected. Dynamic explicit method includes material nonlinearity and also geometrical nonlinearity. It is capable of analyzing post buckling analysis. By changing bulk viscosity between 0 and 0.003 different results were recorded but 0.0015 of bulk viscosity gives us the best result. And also quadratic viscosity of 1.2 which is default value was used. Finally, the required field output and history output was selected.

3.6.5 Boundary condition and Loading

At both ends pin support which is not constrained in longitudinal direction of the column was used. Displacement control method was adopted for loading because of column slenderness. Loading was done for each specimen at different eccentricity so that to draw interaction diagram. Loading speed of -0.004m/sec was used. Around fifteen eccentricities were considered for each specimen.

3.6.6 Meshing

i) Mesh size

Different analysis was done in validation work using different mesh size until the analysis result was conforming to experimental result. So 0.02m mesh size gave the best result which conforms to experimental result and takes reasonable running time for the model. Since dependent instances were used mesh was done for parts.

ii) Element type

For Plain concrete column and steel plate part C3D8R was used which is an 8 nodes linear brick, reduced integration hourglass control and B31 element which is first order three dimensional beam element was used for reinforcement. But T3D2 which is first order three dimensional truss element was used for lateral reinforcement.

Finally, job was created and the result was taken when the analysis was completed. Though stress-strain was checked, only load and displacement curve was collected for different eccentricity in each specimen analysis. This load-displacement data for SRC1 specimen is presented in appendix C. The maximum load and its corresponding displacement were taken for computation of load and moment. Finally, interaction diagram was drawn using computed axial load and moment.

3.7 Development of axial load and moment interaction diagram using simplified method (Nominal stiffness) of EC2.

In a second order analysis based on stiffness, nominal values of the flexural stiffness should be used, taking into account the effect of cracking and material nonlinearity. The following equation enable us to compute magnification factor in which the first order moment is magnified. It is taken from EC2, sec 5.8.7.

$$\delta = \frac{1}{1 - \frac{N_d}{N_B}} \qquad \text{Eqn.3-22,EC-2,(5.30)}$$

$$M_{ED} = \delta * M_{oED} \qquad \text{Eqn.3-23,EC-2,(5.30)}$$

But in this work section capacity of the column is going to be computed based on the material property which is described later. Due to second order effect the capacity of the column will be reduced. So the factor will be used as reduction factor and the equation is changed as follows:

$$M_{ED} = \frac{M_{oED}}{\delta} \qquad \text{Eqn.3-24}$$

Using equation 2-4,2-6,2-7,2-8, buckling load was computed and used it in reduction factor equation. But the way in which M_{oED} and N_{ED} was calculated is described as follows.

$$N_{ED}=\alpha_c b d f_{ck}'+\frac{A_{st}}{2} f_{s'} \mp \frac{A_{st}}{2} f_s \qquad \text{Eqn.3-25}$$

$$M_{oED}=\alpha_c b d f_{ck}'\left(\frac{h}{2}-\beta_c d\right)+\frac{A_{st}}{2} f_{s'}\left(\frac{h}{2}-d'\right)+\frac{A_{st}}{2} f_s\left(d-\frac{h}{2}\right) \qquad \text{Eqn.3-26}$$

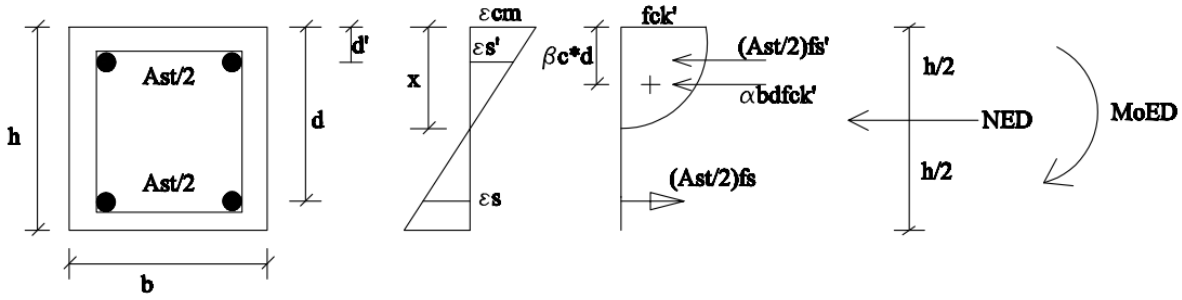

a) Section b) strain c) stress

Figure3. 13: Sectional Stress-strain diagram

Where α_c and β_c depends on stress-strain of the concrete and formulated based on the following stress-strain diagram. It is also derived on EBCS-2, part-2. (Girma zerayohannes,2015).

$$\sigma_c=f_{ck}^{'}\left[1-\left(1-\frac{\varepsilon_{cm}}{\varepsilon_{c2}}\right)^2\right] \qquad \text{for } 0\leq\varepsilon_{cm}\leq\varepsilon_{c2}$$

$$\sigma_c=f_{ck}^{'} \qquad \text{for } \varepsilon_{c2}\leq\varepsilon_{cm}\leq\varepsilon_{cu2}$$

ε_{cm} is compressive strain of concrete at the extreme fiber.

ε_{c2} is compressive strain of concrete at the peak stress and 0.002 was used.

ε_{cu2} is maximum compressive strain of concrete and 0.0035 was used.

In order to compare this simplified method with FEA result, f_{ck}' was used in place of f_{cd} but f_{ck}'=0.85* f_{ck}. Reduction factor was used due to the difference in maximum compressive stress reached in the concrete of flexural member with cylindrical strength of concrete. This difference is occurred because of difference in size and shape of the compressed concrete. (R.Park et al.,1974).

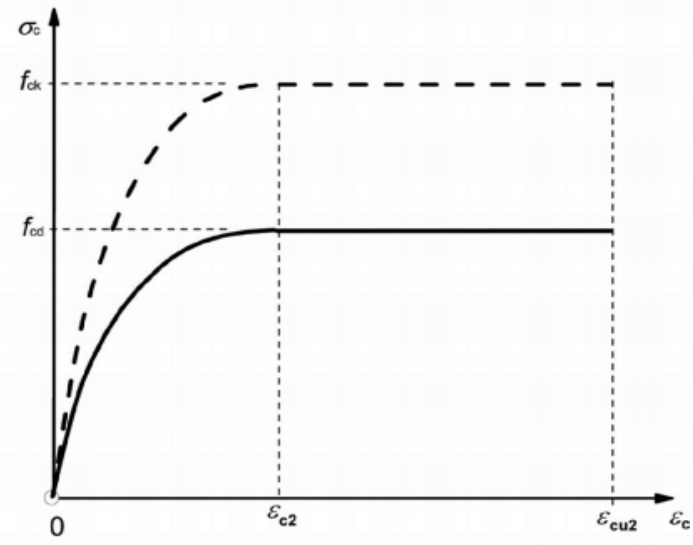

Figure3. 14: parabola rectangular Stress-strain diagram of concrete, EC-2(3.3)

Based on the variation of stress-strain diagram of the concrete and location of neutral axis equation is categorized into three.

i) When $\varepsilon_{cm} \leq \varepsilon_o$ and $x \leq h$

$$\alpha_c = \frac{\varepsilon_{cm}}{12}(6-\varepsilon_{cm})k_x \qquad \text{Eqn.3-27}$$

$$\beta_c = \frac{(8-\varepsilon_{cm})k_x}{4(6-\varepsilon_{cm})} \qquad \text{Eqn.3-28}$$

ii) When $\varepsilon_{cm} > \varepsilon_o$ and $x \leq h$

$$\alpha_c = \frac{(3\varepsilon_{cm}-2)k_x}{3\varepsilon_{cm}} \qquad \text{Eqn.3-29}$$

$$\beta_c = \frac{\varepsilon_{cm}(3\varepsilon_{cm}-4)+2}{2\varepsilon_{cm}(3\varepsilon_{cm}-2)}k_x \qquad \text{Eqn.3-30}$$

iii) When $\varepsilon_{cm} > \varepsilon_o$ and $x > h$

$$\alpha_c = \frac{1}{189}(125+64\varepsilon_{cm}-16\varepsilon_{cm}^2) \qquad \text{Eqn.3-31}$$

$$\beta_c = 0.5-\frac{40}{7}*\left(\frac{(\varepsilon_{cm}-2)^2}{(125+64\varepsilon_{cm}-16\varepsilon_{cm}^2)}\right. \qquad \text{Eqn.3-32}$$

Where K_x is x/d and x is the position of neutral axis

But for steel elasto plastic was used and strain compatibility was used to get the stress of steel.

Using the above illustrated equation excel template was prepared and points for interaction diagram was generated and it is plotted together with FEA result in discussion part and appendix D for each specimen. But before generating points for specimen verifying the template was done by generating the points for short column to draw interaction diagram which is provided on EBSC-2, part-2. (Girma zerayohannes,2015).

CHAPTER FOUR

VALIDATION OF FINITE ELEMENT MODELLING

4.1 Bench mark experiment

Claeson et al. which is done on slender high strength concrete columns subjected to eccentric loading was used as benchmark experiment. Specimen N-B (I) was selected for this thesis to use it as bench mark.

i) Geometrical property

The dimension of the specimen is 200 mm by 200mm and its concrete cover is 15mm.Four longitudinal reinforcements which have 16mm diameter and 8mm diameter for lateral reinforcement.

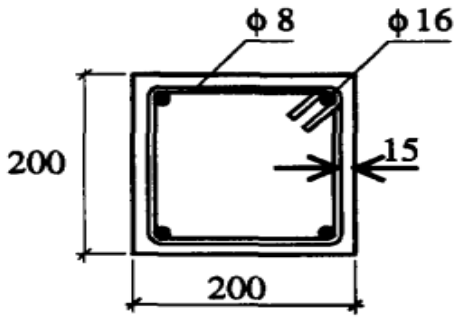

Figure 4. 1: Detail of benchmark experiment specimen

The length of column is 3m and it is pinned at both ends of the column. The eccentricity for axial load is 20mm and spacing of the lateral reinforcement is 130mm.

ii) Concrete property

Normal strength of concrete was used for the specimen. Property of concrete which is used in the column specimen is described as follows:

Table 4. 1: Composition of concrete mixes

Water (Kg/m^3)	189
Portland cement (Kg/m^3)	370
Sand (Kg/m^3)	980
Crushed stone (gneiss) 8/16 (Kg/m^3)	870

Table 4. 2: properties of hardened concrete at 28 days (Mean strength of three specimens)

Specimen	**$f_{c,cube}$(Mpa)**	**$f_{c,cyl}$(Mpa)**	**$f_{t,split}$(Mpa)**	**E_o(Gpa)**	**E_c(Gpa)**
N-B(I)	43	33	3.7	26	25

iii) Steel property

Property of steel reinforcement was tabulated in research methodology table 3.3.

iv) Experimental result

The maximum load is 990KN and its corresponding deflection is 22mm.Load displacement curve is also plotted together with finite element results in Fig 4.2.

4.2 FE result

Before starting modelling of the research specimen the validation work was done in order to decide on different parameters. So using the method which is described in chapter three the above described specimen was modeled. By changing loading speed, bulk viscosity and mesh size different analysis was done and also load-displacement curve was recorded. But three of them are selected and presented here together with the experimental curve. For illustration purpose the analysis results are categorized as Valid-1, Valid-2 and Valid-3. For example, Valid-1 is the slender reinforced concrete column modelled with mesh size of 20mm, bulk viscosity of 0 and compressive loading of 0.0015m/sec. As it is shown in Fig 4.2, there is difference in ascending of load-displacement curve of FEA and experimental. Since elastic modulus is the slope of stress-strain curve, the difference is created due to difference in elastic modulus of FEA and experimental. As it is mentioned in research methodology, table 3.2 elastic modulus for FEA was 33.5937Gpa which is steep but for experimental 26Gpa & 25Gpa which is listed in the table 4.2.

Table 4. 3: Categorization of load displacement curve

Catagory	Mesh size	Bulk viscosity	Speed(m/sec)
Valid-1	20	0	-0.0015
Valid-2	20	0.003	-0.004
Valid-3	20	0.0015	-0.004

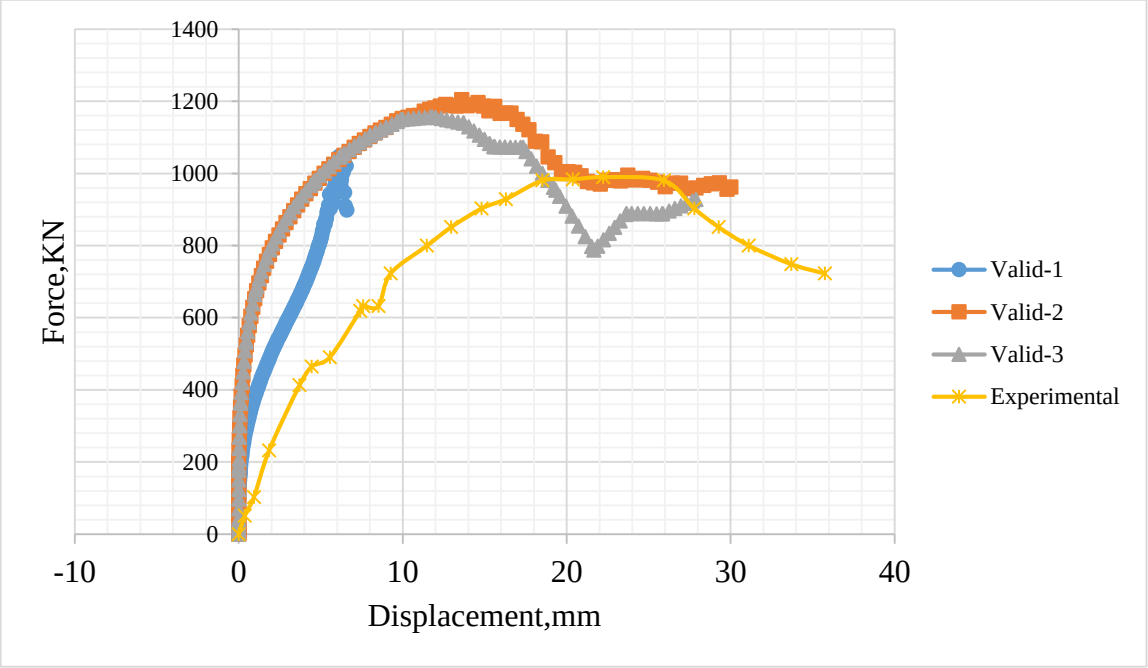

Figure 4. 2: Comparison of FE load-displacement curve with experimental

Table 4. 4: FEA results and comparison with experimental

Category	Maximum load(KN)	F_{exp}/F_{FEA}
Experimental	990	1
Valid-1(FE)	1047.34	0.9452
Valid-2(FE)	1204.33	0.822
Valid-3 (FE)	1156.8	0.85581

Figure 4.2 and table 4.4 shows that the category of Valid-1 have the load which is nearest to experimental but the corresponding displacement is very small and far from the experimental. But Valid-3 is best conform to the experimental curve. The maximum load of valid-3 is 1156.8KN and the maximum load of experimental is 990KN.So the experimental is 85.581% of the maximum load of Valid-3. This indicate that FE result well conformed to the experimental result.

CHAPTER FIVE

RESULT AND DISCUSSION

Since the FE result was well conformed with the experimental result in the previous chapter, the specimen result which is presented below is assumed to represent the behavior of the column well.

5.1 Results

The analysis result which was modelled using the method described in research methodology are presented below. The data which was taken from the software was load displacement curve but under this topic only interaction diagram is plotted and presented below. The load displacement curve for SRC1 specimen at different eccentricities are presented in appendix C but for the purpose of illustration the load displacement curve for SRC1 at axial load 10mm from the center column is plotted below.

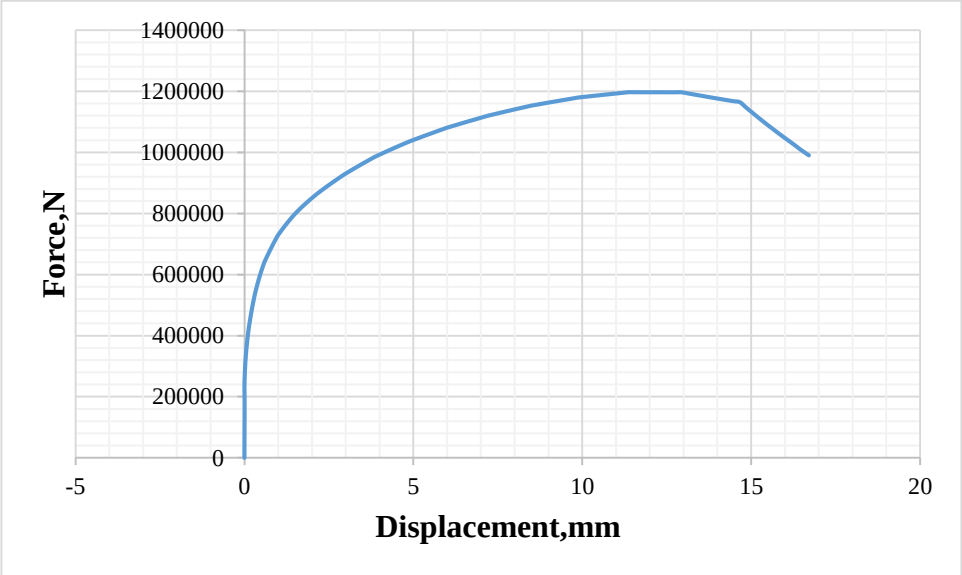

Figure 5. 1: Load-displacement curve for SRC1 column and axial load at, e=10mm.

For each specimen the maximum load and corresponding displacement was taken to plot axial load and moment interaction diagram. For example, from Figure 5.1 maximum load is 1196910N and displacement is 11. 3716mm.This is done for all specimen at different eccentricities and it is tabulated and plotted as follows:

Table 5. 1: Axial load and moment for SRC1

Force(N)	Force(KN)	Δ(mm)	e(mm)	e+Δ(m)	M=F(e+Δ)
1356260	1356.26	0	0	0	0
1196910	1196.91	11.3716	10	0.0213716	25.57988
1066370	1066.37	14.1933	20	0.0341933	36.46271
835670	835.67	25.1304	30	0.0551304	46.07082
774024	774.024	20.9338	40	0.0609338	47.16422
617640	617.64	23.9412	50	0.0739412	45.66906
568529	568.529	19.6088	60	0.0796088	45.25988
461226	461.226	25.3469	70	0.0953469	43.97645
430819	430.819	21.1345	80	0.1011345	43.57066
371229	371.229	23.68	90	0.11368	42.20131
315741	315.741	20.8916	110	0.1308916	41.32786
251086	251.086	24.8036	120	0.1448036	36.35816
230099	230.099	24.9041	130	0.1549041	35.64328
210903	210.903	23.8936	140	0.1638936	34.56565
-128361	-128.361	0	0	0	0

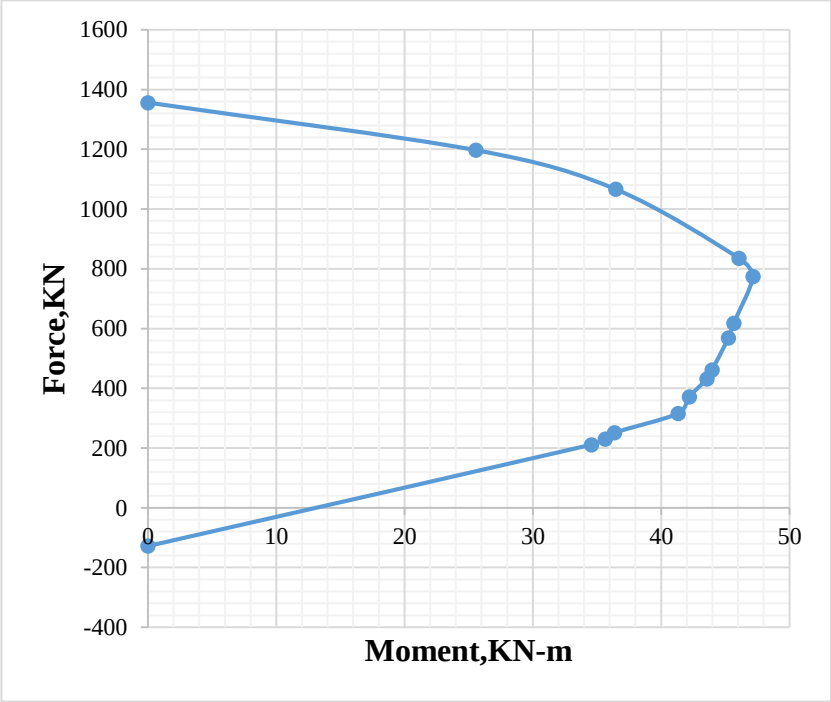

Figure 5. 2: Axial load-moment interaction diagram for SRC1.

For other specimen the table is tabulated in appendix B but the diagram is plotted as follows:

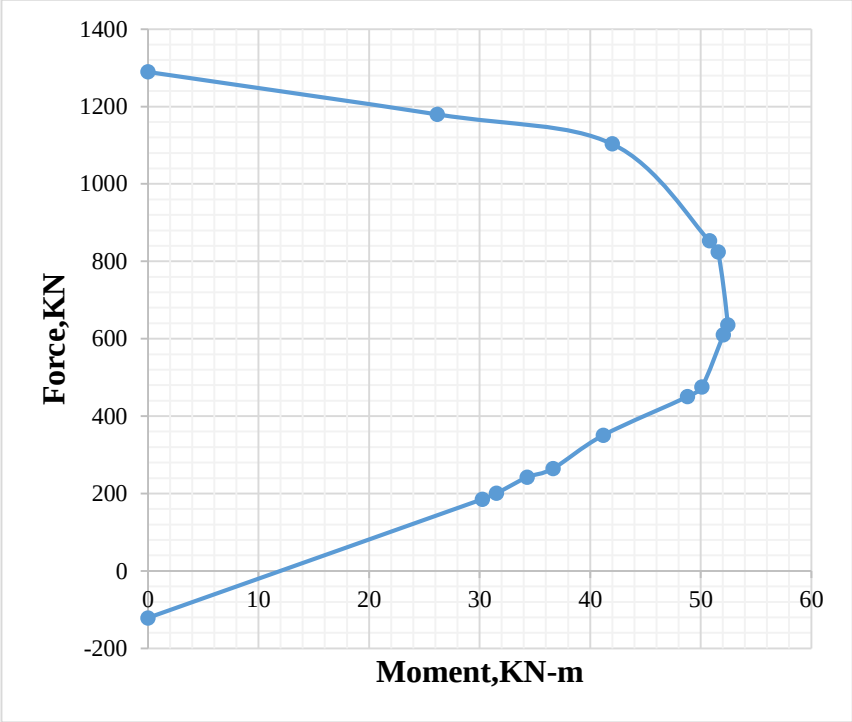

Figure 5. 3: Axial load-moment interaction diagram for SRC2.

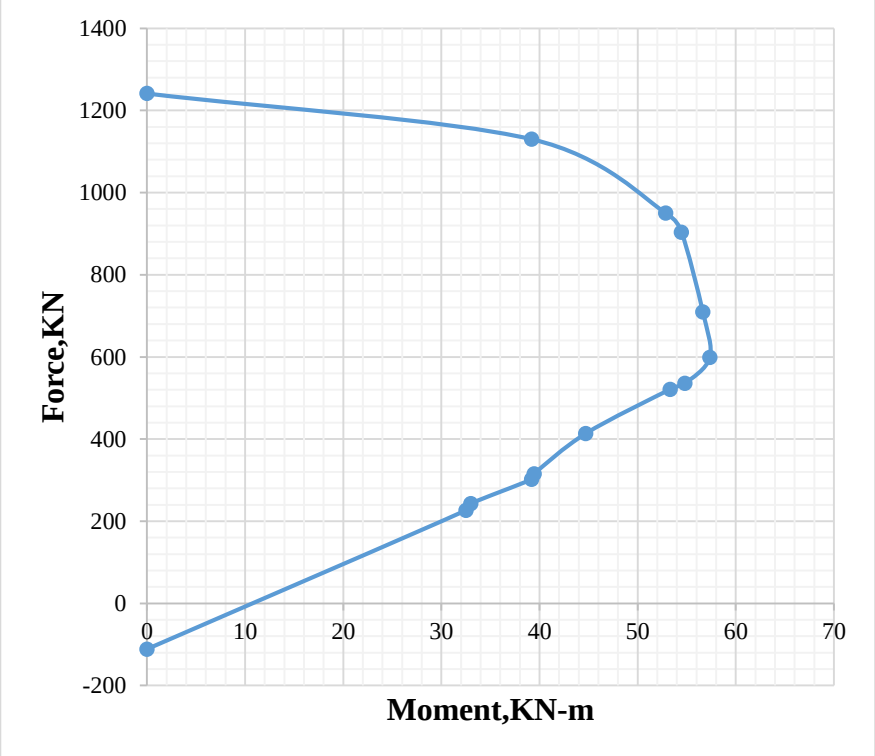

Figure 5. 4: Axial load-moment interaction diagram for SRC3.

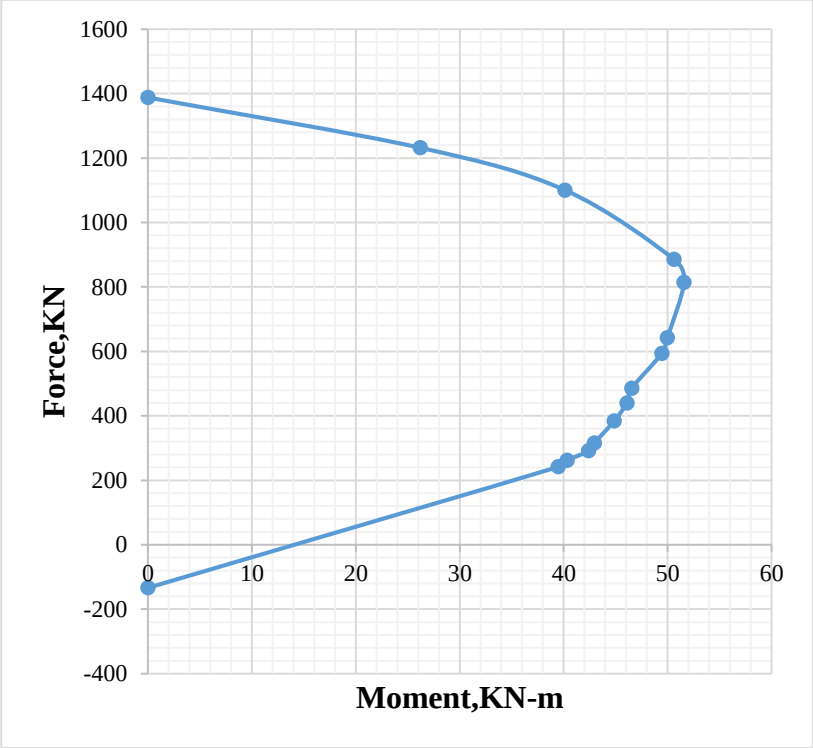

Figure 5. 5: Axial load-moment interaction diagram for SRC4.

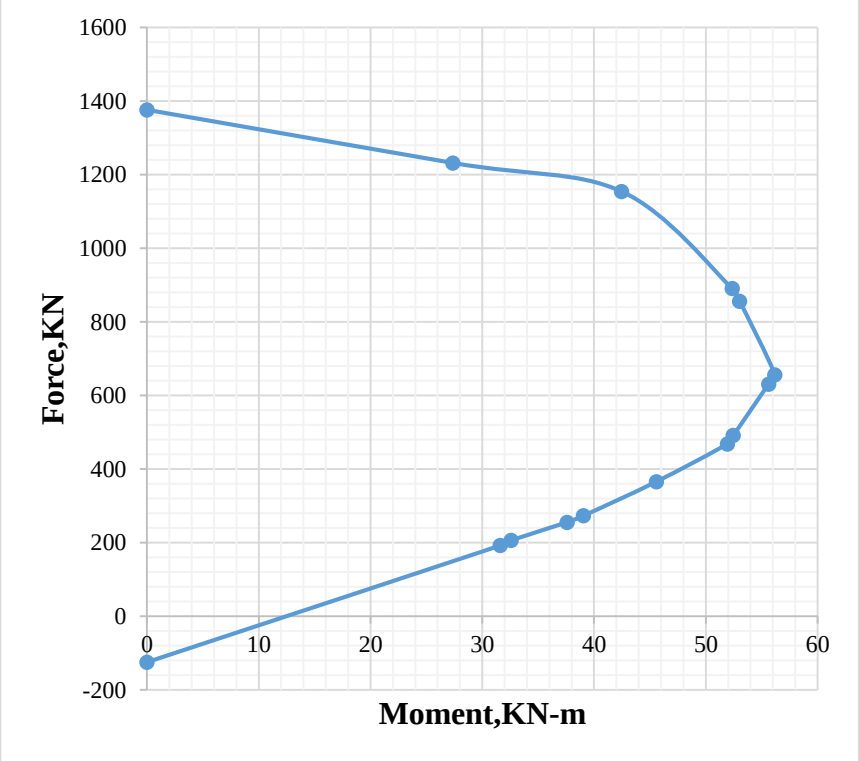

Figure 5. 6: Axial load-moment interaction diagram for SRC5.

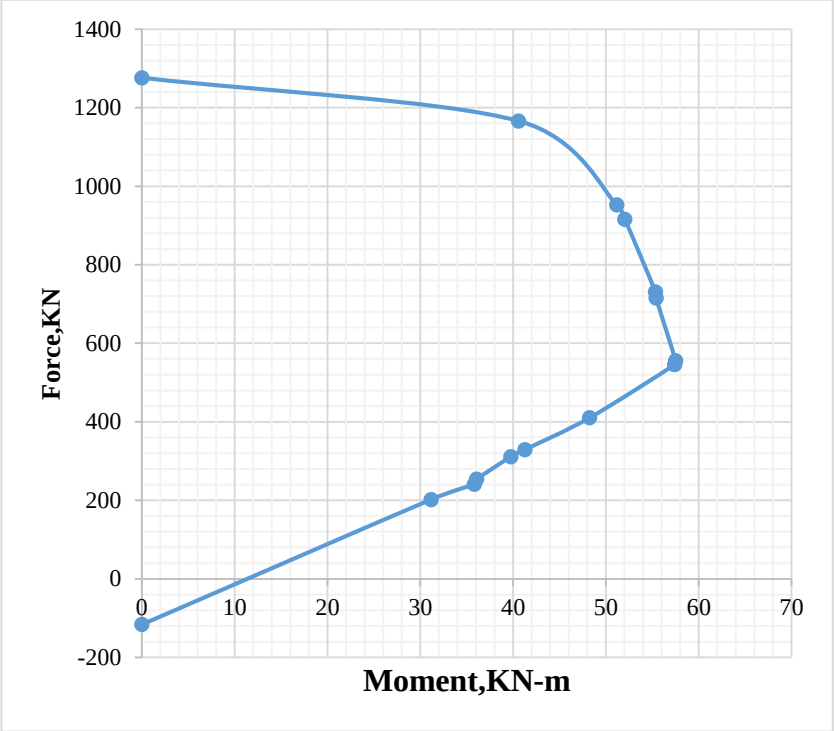

Figure 5. 7: Axial load-moment interaction diagram for SRC6.

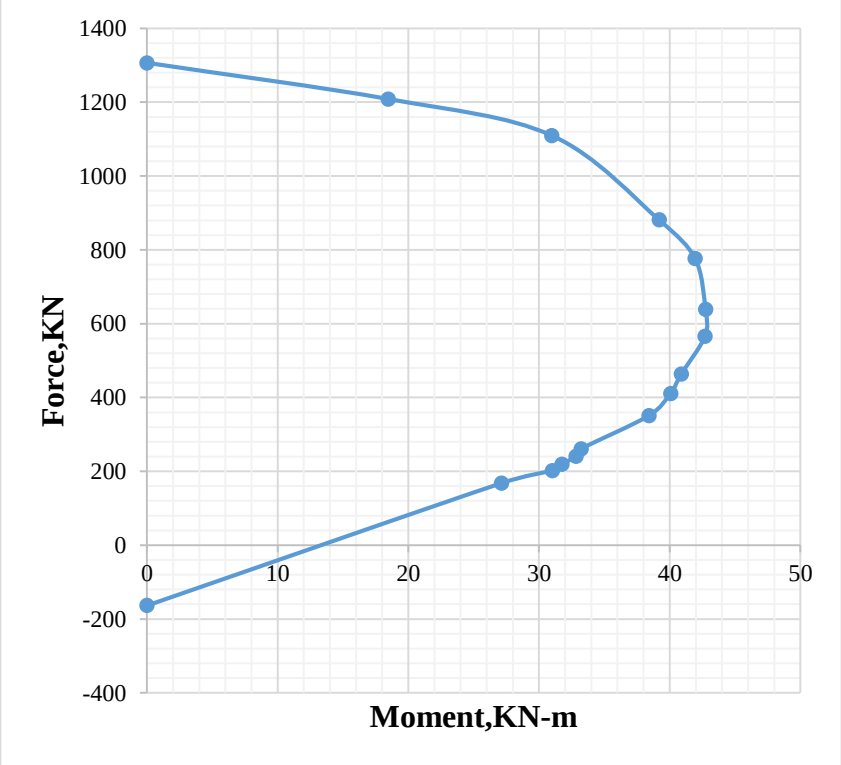

Figure 5. 8: Axial load-moment interaction diagram for RRC1.

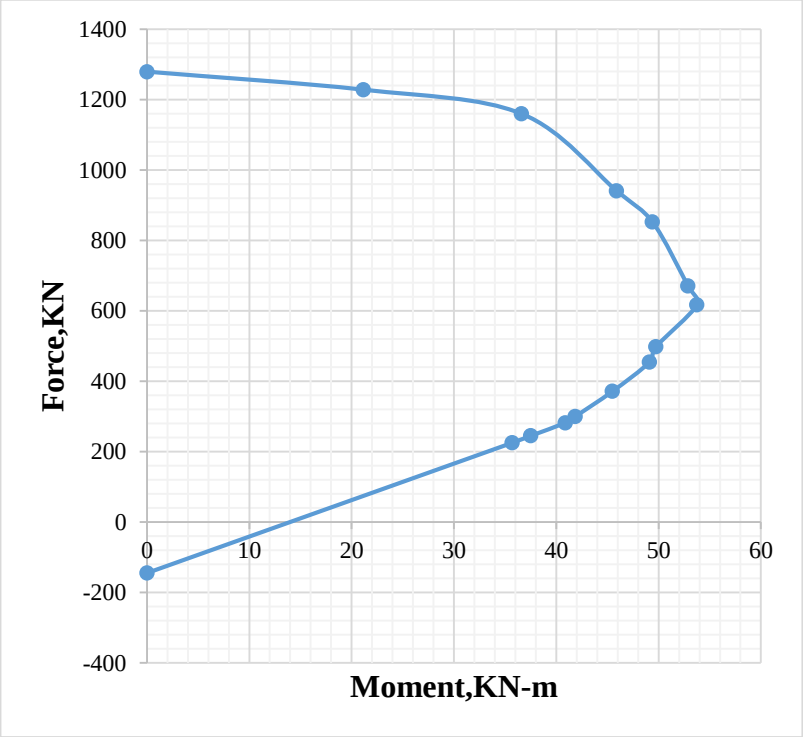

Figure 5. 9: Axial load-moment interaction diagram for RRC2.

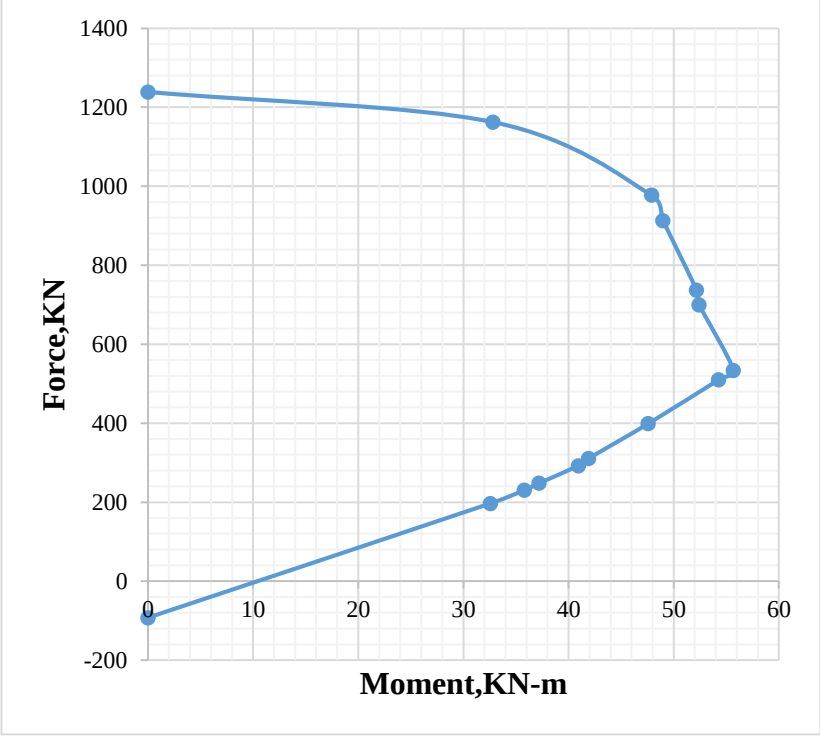

Figure 5. 10: Axial load-moment interaction diagram for RRC3.

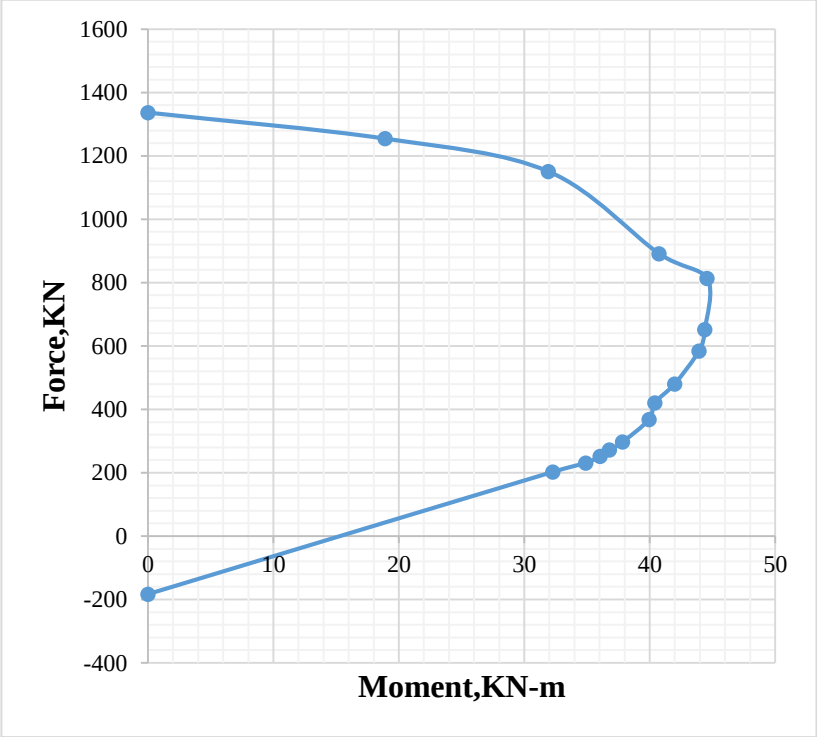

Figure 5. 11: Axial load-moment interaction diagram for RRC4.

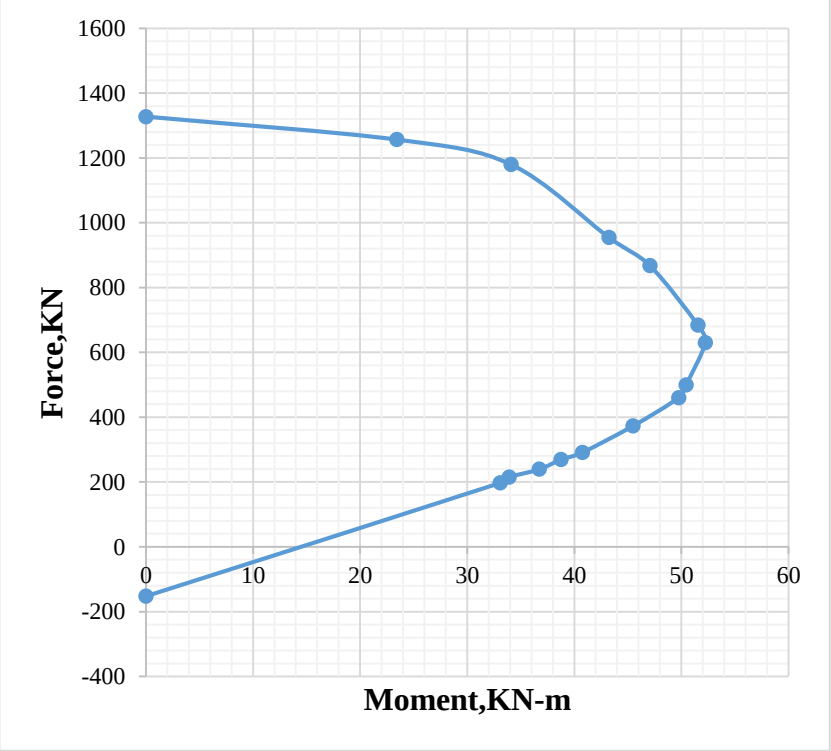

Figure 5. 12: Axial load-moment interaction diagram for RRC5.

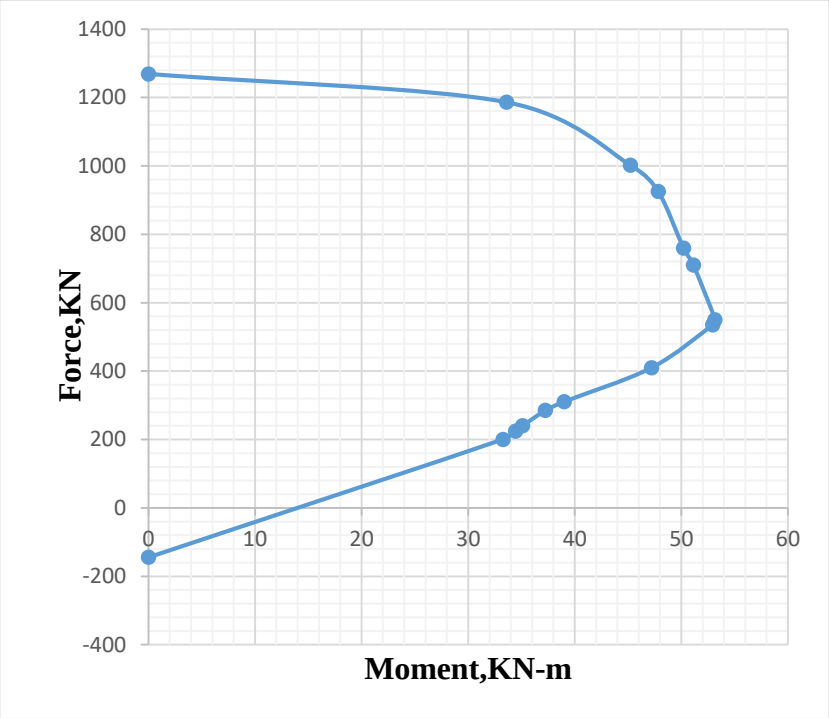

Figure 5. 13: Axial load-moment interaction diagram for RRC6.

5.2 Discussion

As shown in all diagrams above as the eccentricities increased the load is decreased in slow manner but the moment increases rapidly. Especially in compression control zone the slope of the curve is gentle which indicate that the difference in compression failure load for two different eccentricities is small.

The effect of slenderness ratio on uniaxial interaction diagram

As it is well known and indicated in the Fig5.14 below, the increase in slenderness ratio decreases the capacity of pure axial column. Since the analysis was done nonlinear, the second order effect was also included. As slenderness ratio increases the second order effect also increases and result in large displacement. This increase in displacement also increase the moment at the mid height of the column. This is occurred when the load is approach to balanced load. For example, for first specimen(SRC1) with slenderness ratio of 60.62 the balanced axial load capacity and moment capacity is774.024KN and 47.1642KN-m respectively.

But for second specimen(SRC2) with slenderness ratio of 80.54 it is 635.928KN and 52.4527KN-m. The reduction in axial capacity is 17.84% and the increase in moment is 11.21%. However, as amount of steel increased the stability of the column is increased and second order effect is reduced. As it is illustrated in Fig 5.14 below, for high eccentricity and tension control zone the capacity reinforced concrete column is approximated to each other.

The illustrated figure below is only for square reinforced concrete column but rectangular reinforced concrete column is illustrated in appendix D.

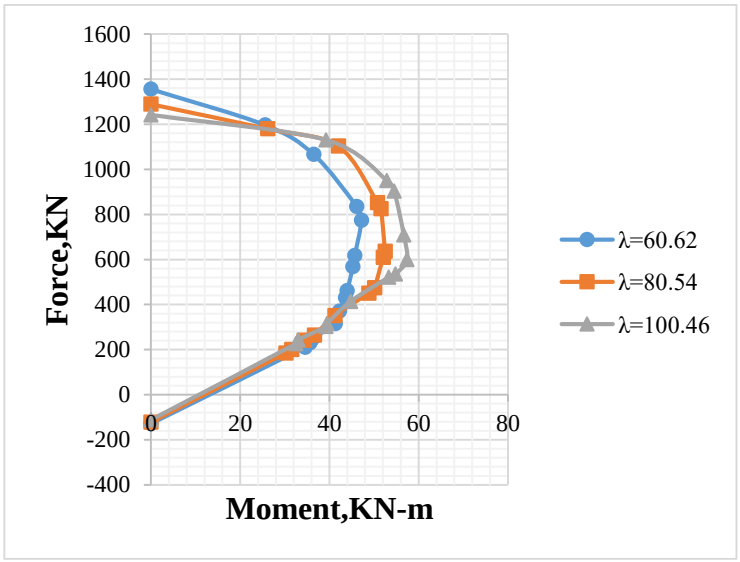

a) For square column with ρ=0.01223

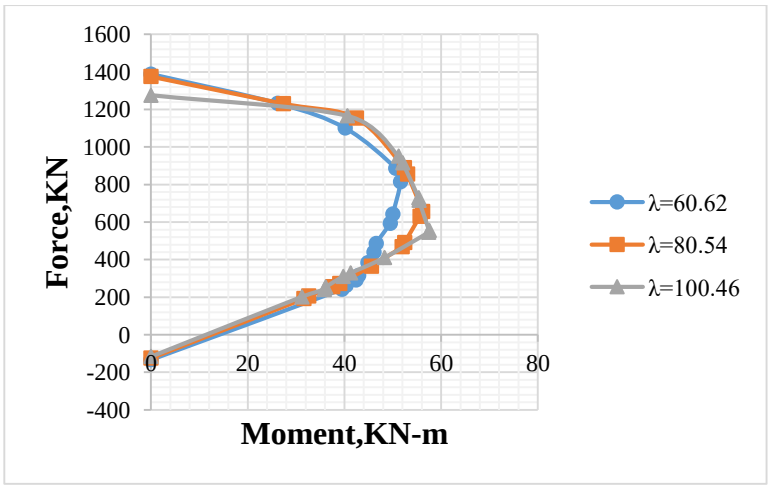

a) For square column with ρ=0.01664

Figure 5. 14: Comparison of Axial load-moment interaction diagram based on slenderness ratio.

The effect of steel reinforcement on uniaxial interaction diagram

As it is shown in the Fig5.15, increasing the amount of steel increases the compression, balanced and also tension failure load. But as the slenderness ratio increased in tension control zone, the effect of increasing amount of steel is insignificant. This is caused due to premature or instability failure. As the eccentricity approach to large value and slenderness also increased, the buckling of the column will be very large and result in premature failure.

The illustrated figure is only for square RC column but rectangular RC column is illustrated in Appendix D.

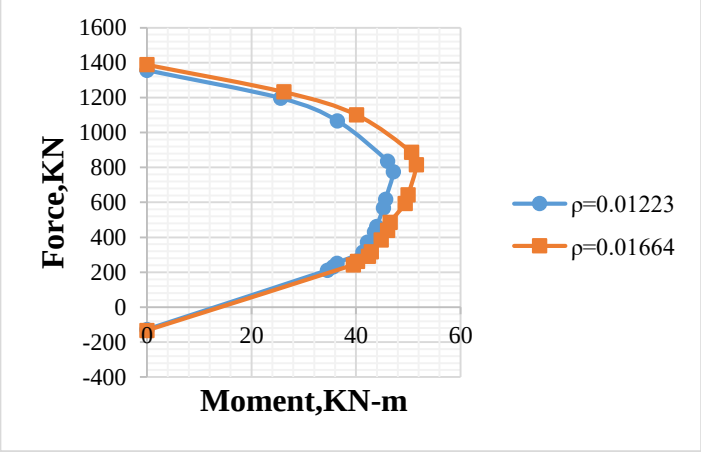

a) For square column with λ=60.62

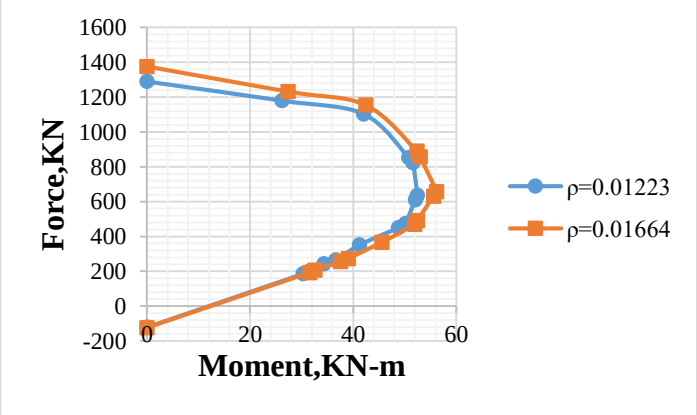

b) For square column with λ=80.54

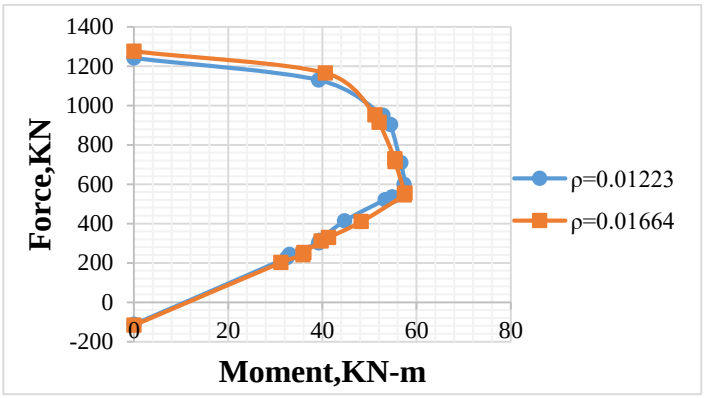

c) For square column with λ=100.46

Figure 5. 15: Comparison of Axial load-moment interaction diagram based on steel ratio.

The effect of shape of column on uniaxial interaction diagram

The shape of the column has effect on the capacity of slender reinforced concrete column. In this thesis only square and rectangular reinforced concrete column which have equivalent area was considered. For rectangular column the eccentricity was considered in the minor axis direction so that the column will be uniaxial. The capacity of square reinforced concrete column is larger than rectangular one. But with increasing slenderness ratio the effect of the shape is diminishing as it illustrated below in fig 5.16. The effect is the same with the increase in amount of steel.

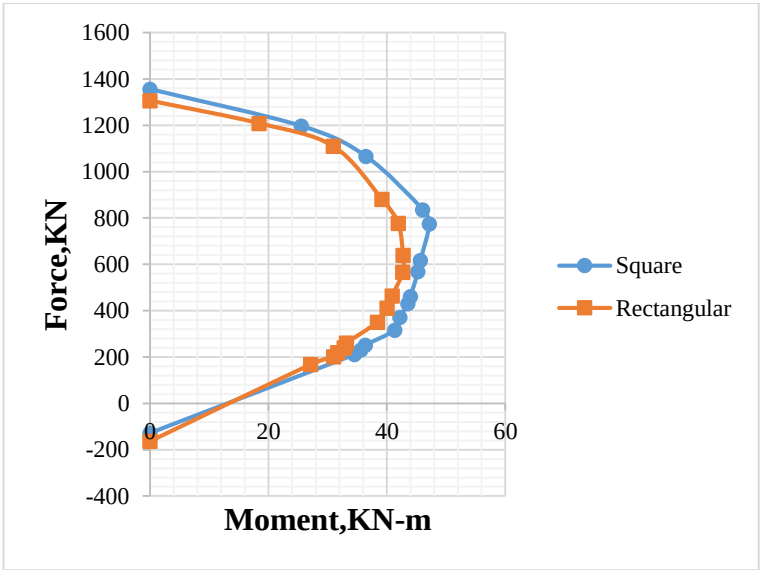

a) Column with ρ=0.01223 and λ=60.6

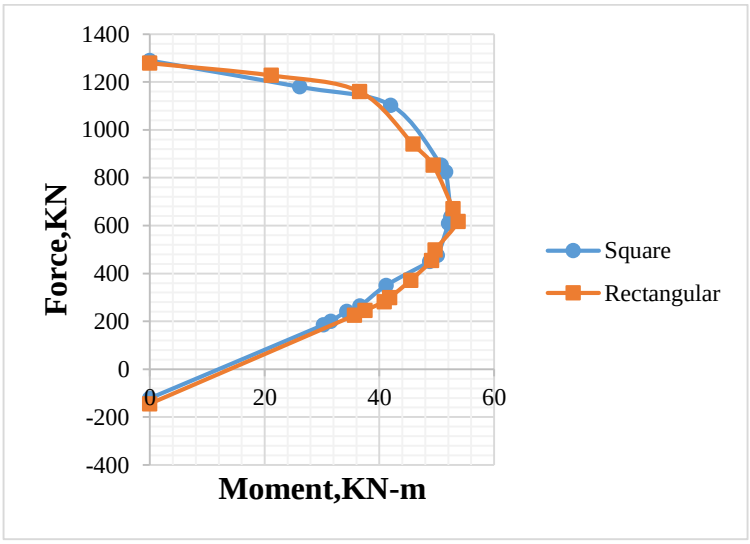

b) Column with ρ=0.01223 and λ=80.5

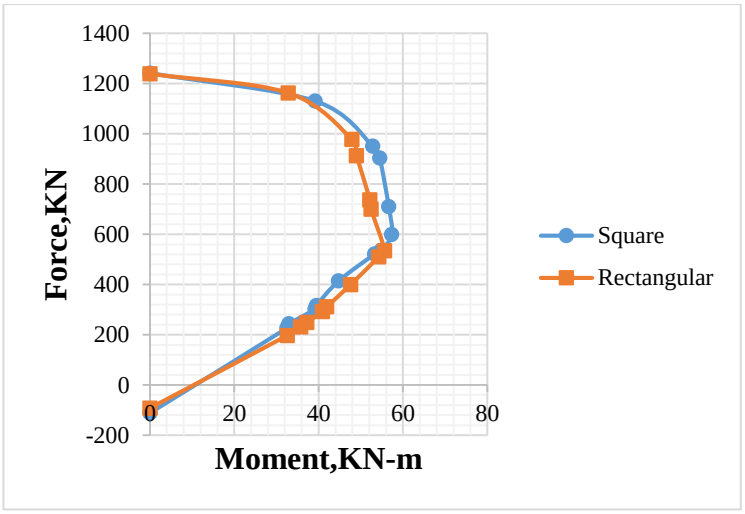

c) Column with ρ=0.01223 and λ=100.46

Figure 5. 16: Comparison of Axial load-moment interaction diagram based on shape of the column.

Comparison of FEA result with Nominal Stiffness Method (NSM)

As it is described in research methodology, axial load and moment interaction diagram is also prepared using nominal stiffness method. It is plotted together with FEA result in the following figure and also in appendix D. In preparing axial load-moment interaction diagram using nominal stiffness method the material nonlinearity that was considered only in ascending branch of compressive stress-strain diagram of concrete was used but in FEA the nonlinearity throughout the diagram was considered. In NSM the section capacity was first

determined by ignoring the tensile strength of concrete and the reduction factor for moment capacity to account for the second order effect was used. But in FEA tensile strength of concrete was used using tension stiffening effect. And also in nominal stiffness method for second order analysis the effect of cracking is accounted for crack location of maximum moment but in FEA analysis the crack variation throughout column length is considered. Geometrical nonlinearity is better approximated in FEA than nominal stiffness method. The tensile load which was used in NSM was tensile force of reinforcement steel. Because of the above described reason the two method gives us different result and it is illustrated below in Fig5.17. As the slenderness ratio increases nominal stiffness method(NSM) underestimate the capacity of slender column.

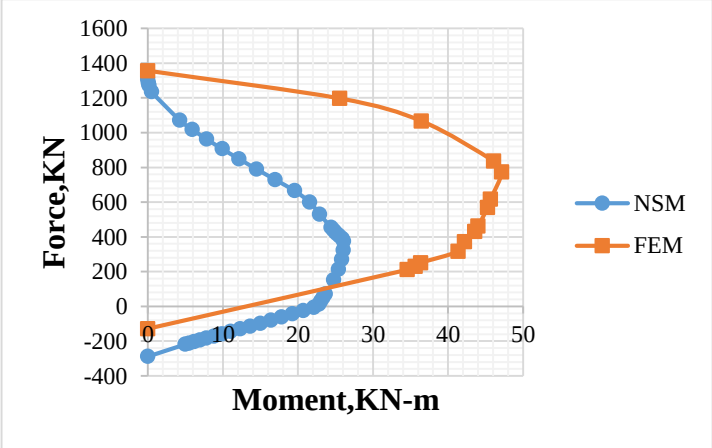

a) Square column with ρ=0.01223 and λ=60.62(SRC1)

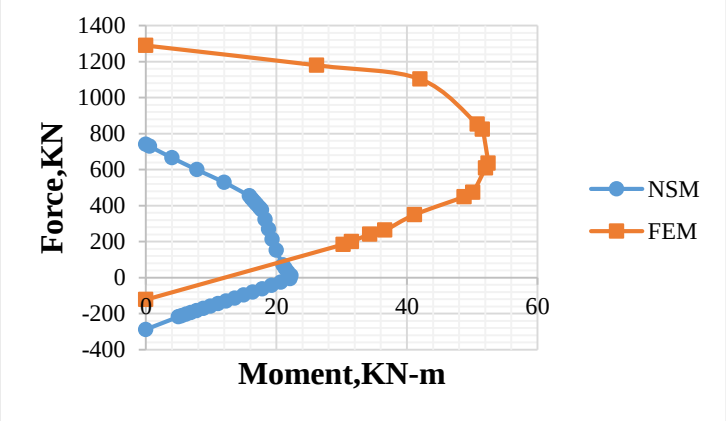

b) Square column with ρ=0.01223 and λ=80.54(SRC2)

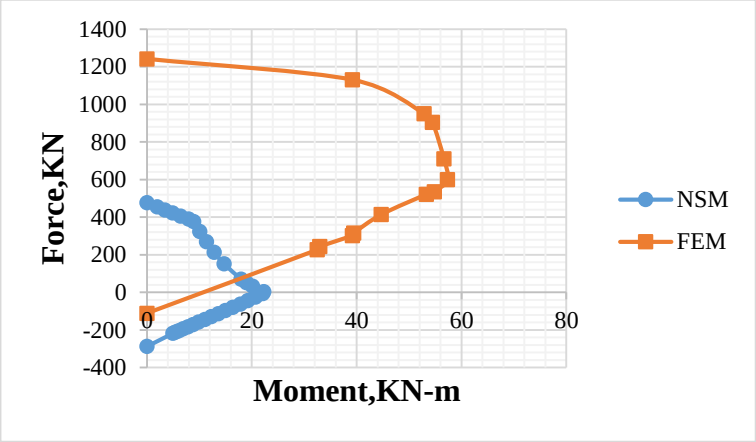

b) Square column with ρ=0.01223 and λ=100.46(SRC3)

Figure 5. 17: Comparison of Axial load-moment interaction diagram based on FE result and nominal stiffness method.

In order to prevent redundancy, the interaction diagram which is prepared using nominal stiffness method is plotted only together with FEA result for illustration purpose. So other comparison charts are plotted in appendix D in addition to the above charts.

CHAPTER SIX

CONCLUSION AND RECOMMENDATION

6.1 Conclusion

First Literature review was done to decide on the title and then planning was done to solve the identified problem. According to the planning the software training was held and validation was done in which experimental result was 85.581% of FEA result. Considering the capability of the software and the number of the variable the specimens was selected. Concrete damage plasticity for concrete and metal plasticity for steel was used. Material properties which suits the selected material model and also used as input data for modeling of the specimen was prepared. Density and poison ratio of 7850Kg/m^3 and 0.3 was used for steel but for concrete 2400Kg/m^3 and 0.2 was used respectively. Subsequently, modeling and analysis of slender RC column was done. Based on the analysis results the axial load-moment interaction diagram was prepared for all specimen.

The diagram reveals that as slenderness ratio increases the balanced moment also increases but the corresponding axial load was decreases. For example, as slenderness ratio increases from 60.62 for SRC1 to 80.54 for SRC2 the balanced axial load capacity reduces with 17.84% and moment increases with 11.21%. But increasing amount of steel to the column increase the stability of the column and reduce difference in balanced moment due to slenderness ratio. For the same slenderness ratio increasing the amount of steel also increase all compression failure load, balanced failure load and tension failure load. And also the capacity of square slender RC column is larger than rectangular slender RC column with equivalent cross-section. But increasing the slenderness ratio reduces the difference in the capacity of square slender RC column and rectangular slender RC column.

Finally, axial load-moment interaction diagram was prepared for all specimens using nominal stiffness method and comparison was made with FEA results. It shows that the capacity of the column that result from FEA was greater than the nominal stiffness method.

6.2 Recommendation

In this thesis construction of interaction diagram using nonlinear FEA software which includes only material nonlinearity, geometric nonlinearity, cracking effect and tension stiffening effect. But due to different types of loading on the column and others factors it is clear that further and extensive research work needs to be done in order to know the behavior of slender RC column very well.

The following are among the areas of slender RC column which needs further research.

1.Construction of uniaxial interaction diagram for slender RC column using nonlinear FEA software including creep effect in addition to the factor considered in this research.

2.Construction of biaxial interaction diagram for slender RC column using nonlinear FEA software.

3.Adding the effect of confinement to the above mentioned areas.

REFERENCES

Abaqus CAE user guide version 6.13(2013). Pawtucket(RI);Hibbit, Karlsson and Sorensen.

Abaqus release note version 6.13(2013). Pawtucket(RI);Hibbit, Karlsson and Sorensen.

Abaqus theory version 6.13(2013). Pawtucket(RI);Hibbit, Karlsson and Sorensen.

Abaqus analysis-2 user's manual version 6.13(2013). Pawtucket(RI);Hibbit, Karlsson and Sorensen.

Abaqus analysis-3 user's manual version 6.13(2013). Pawtucket(RI);Hibbit, Karlsson and Sorensen.

Alfarah B, Lopez-Almensa F,Oller S(2017).New methodology for calculating damage variables evolution in plastic damage model for RC structures. Engineering structures.132:70-86.

ACI Committee 318. (1989). Commentary on the building code requirements for reinforced concrete (ACI318R-89), American Concrete Institute, Farmington Hills, MI,369pp.

Bazant Z.P and Kwon Y.W (1994). Failure of slender and stocky reinforced concrete columns: test of size effect. Material and Structures.27:79-90.

Cleason C and Gylltoft K (1998). Slender high strength concrete column subjected to eccentric loading. Journal of structural Engineering.124(3):233-240.

Euro code-2(2002). Design of concrete structure, Part-1: Generals rules and rules for building. Brussels.

Girma Zerayohannes (2015). Ethiopian Building Code Standard Two part 2: Design aids for Reinforced Concrete Sections on the bases of EN EBCS2, Ministry of works and urban development, Addis Ababa.

Hordijk DA (1992). Tensile and tensile fatigue behavior of the concrete: experiments, modelling and analysis. Heron.37(1):3-79.

Kabtamu G. (2012). Master thesis on Approximate uniaxial interaction diagram for slender column using second order formula from EBCS-2, 1995.Addis Ababa, Ethiopia.

Kim J.K and Kwak H.G (2006). Nonlinear behavior of slender RC columns (1). Numerical formulation. Construction and Building material.20:527-537.

Kim J.K and Kwak H.G (2006). Nonlinear behavior of slender RC columns (2). Introduction of design formula. Construction and Building material.20:538-553.

Kim J.K and Yang J.K (1995). Buckling behavior of slender high strength concrete columns. Engineering structures.17(1).

MacGregor J.G, Breen J.E, Pfrang E.O (1970). Design of slender concrete column. ACI Journal.67(2):6-28.

MacGregor J.G and Wight J.K (2005). Reinforced concrete mechanics and design.6th edition. United State of America: New Jersey.

Mirza S.A (1990). Flexural Stiffness of Rectangular Reinforced Concrete Columns. ACI Structural Journal.87(4):425-434.

Nessa Y.N (2015). Master thesis on second order FE element analysis of axially loaded concrete members according to Euro code-2. Stockholm, Sweden.

Nguyen GD, Korsunsky A(2008).Development of an approach to constitutive modelling of concrete :damage coupled with plasticity. International Journal of Solid structures.45(20):483-501.

Park R and Paulay T (1974). Reinforced Concrete Structures. Christchurch. New Zealand.

Rodrigues E.A, Manzoli O.L, Bitencourt jr L.A.G, Dos prazeres,P.G.C. and BitencourtT.N(2015).Failure behavior modelling of slender reinforced concrete columns subjected to eccentric load. Latin America Journal of Solids and Structures.12:520-541.

White D.W and Hajjar J.F (1991). Application of second order elastic analysis in LRFD: Research to practice. Engineering Journal. (AISC).28(4):133-148.

APPENDIX A

MATERIAL PROPERTY

A.1 Concrete properties

Table A. 1: Compressive Stress-Total strain of concrete

ε_c	σ_c
0	0
0.00025	8.385989087
0.000518236	16.40000908
0.000768236	22.92087218
0.001018236	28.49497769
0.001268236	33.08982621
0.001518236	36.67141362
0.001768236	39.20414302
0.002018236	40.65073031
0.002213406	41
0.002268236	40.97210312
0.002518236	40.12729218
0.002768236	38.07331491
0.003018236	34.7650501
0.003268236	30.15510332
0.0035	24.67533528

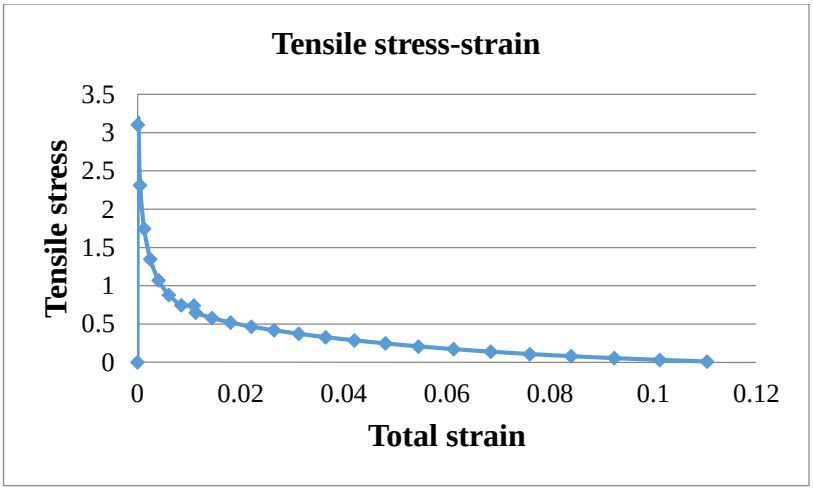

Figure A. 1: Tensile stress-strain

Table A. 2: Stress-crushing strain

σ_c	ε_c^{ch}
16.4	0
22.9209	8.6E-05
28.495	0.00017
33.0898	0.00028
36.6714	0.00043
39.2041	0.0006
40.6507	0.00081
41	0.00099
40.9721	0.00105
40.1273	0.00132
38.0733	0.00163
34.7651	0.00198
30.1551	0.00237
24.6753	0.00277

Table A. 3: Concrete damage variable, dc.

d_c	ε_c^{ch}
0	0
6.1E-06	3.7E-07
0.0005	3E-05
0.00145	8.6E-05
0.00293	0.00017
0.00502	0.00028
0.00782	0.00043
0.01146	0.0006
0.01608	0.00081
0.02048	0.00099
0.02185	0.00105
0.02893	0.00132
0.03751	0.00163
0.04778	0.00198
0.05992	0.00237
0.073	0.00277

Table A. 4: Tensile Stress-Total strain of concrete

εt	ϭt
0	0
0.000100749	3.102944186
0.000500749	2.314373525
0.001300749	1.745642164
0.002500749	1.346136698
0.004100749	1.070073784
0.006100749	0.880050468
0.008500749	0.747518165
0.010920749	0.742000304
0.011300749	0.651826143
0.014500749	0.578746068
0.018100749	0.518950703
0.022100749	0.46666584
0.026500749	0.418573499
0.031300749	0.37297102
0.036500749	0.329156649
0.042100749	0.287000112
0.048100749	0.246656052
0.054500749	0.208382912
0.061300749	0.172436569
0.068500749	0.139014747
0.076100749	0.108234376
0.084100749	0.080129036
0.092500749	0.054657605
0.101300749	0.031718189
0.110500749	0.011163613

Table A. 5: Tensile stress-cracking strain of concrete

Ϭt	εcr
3.102944186	0
2.314373525	0.000433631
1.745642164	0.001250124
1.346136698	0.00246171
1.070073784	0.004069716
0.880050468	0.006075227
0.747518165	0.00847907
0.742000304	0.01089923
0.651826143	0.011281845
0.578746068	0.014483965
0.518950703	0.018085699
0.46666584	0.022087215
0.418573499	0.02648861
0.37297102	0.031289932
0.329156649	0.036491203
0.287000112	0.042092426
0.246656052	0.048093596
0.208382912	0.054494705
0.172436569	0.061295748
0.139014747	0.068496717
0.108234376	0.07609761
0.080129036	0.084098425
0.054657605	0.092499164
0.031718189	0.101299829
0.011163613	0.110500425

Table A. 6: Tensile damage variables-cracking strain of concrete

dt	εcr
0	0
0.005869	1.1E-05
0.228809	0.00043
0.563577	0.00125
0.827948	0.00246
0.952659	0.00407
0.990755	0.00608

A.2 Steel properties

Table A. 7: Tensile stress-strain of longitudinal reinforcement

et	fy
0	0
0.0030725	636
0.005	636
0.022	636
0.027	646.54816
0.032	656.39776
0.037	665.54882
0.042	674.00131
0.047	681.75526
0.052	688.81065
0.057	695.16749
0.062	700.82577
0.067	705.7855
0.072	710.04668
0.077	713.6093
0.082	716.47337
0.087	718.63889
0.092	720.10585
0.097	720.87426
0.1	721

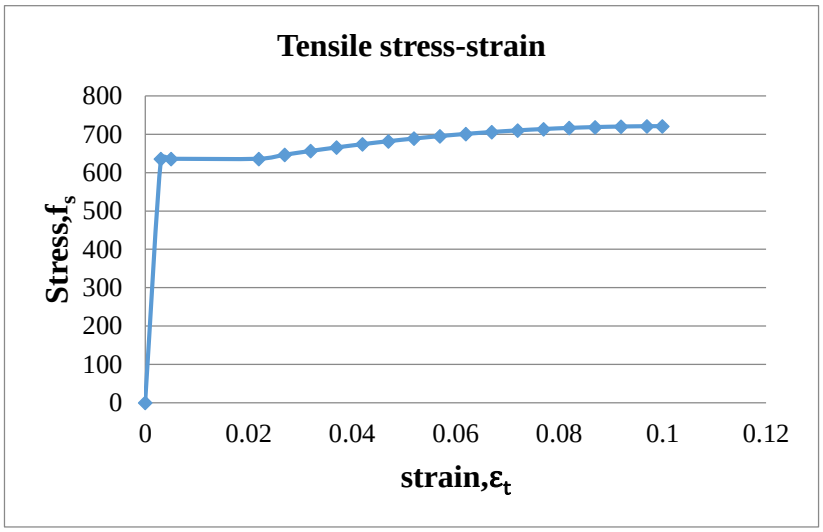

Figure A. 2: Tensile stress-strain of longitudinal reinforcement

Table A. 8: Tensile stress-strain of lateral reinforcement

εt	fy
0	0
0.002108597	466
0.005	466
0.04	466
0.045	484.64844
0.05	502.09375
0.055	518.33594
0.06	533.375
0.065	547.21094
0.07	559.84375
0.075	571.27344
0.08	581.5
0.085	590.52344
0.09	598.34375
0.095	604.96094
0.1	610.375
0.105	614.58594
0.11	617.59375
0.115	619.39844
0.12	620

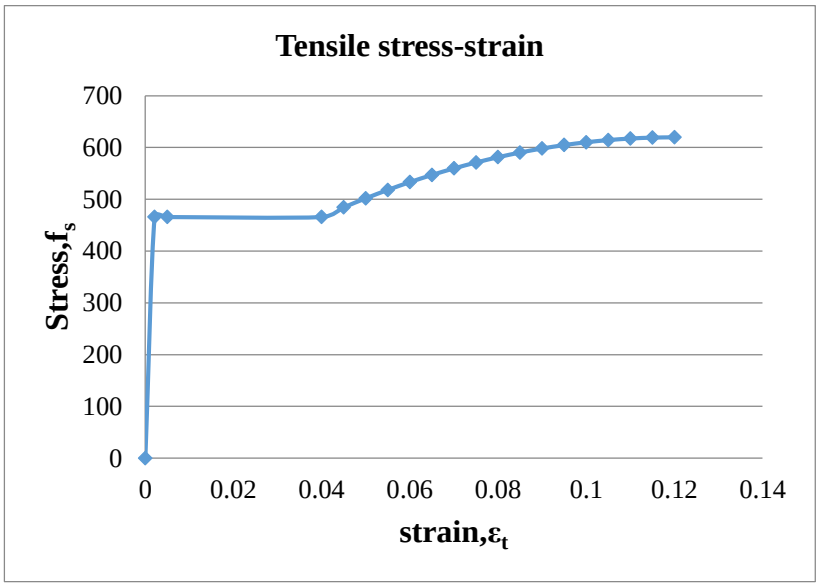

Figure A. 3: Tensile stress-strain of lateral reinforcement

APPENDIX B

AXIAL LOAD AND MOMENT INTERACTION TABLES

Table B. 1: Axial load and moment for SRC2

Force(N)	Force(KN)	Δ(mm)	e(mm)	e+Δ(m)	M=F(e+Δ)
1289530	1289.53	0	0	0	0
1179880	1179.88	12.1755	10	0.0221755	26.16443
1103330	1103.33	18.0734	20	0.0380734	42.00752
852841	852.841	29.5578	30	0.0595578	50.79333
824498	824.498	22.5659	40	0.0625659	51.58546
635928	635.928	32.4822	50	0.0824822	52.45274
609957	609.957	25.3508	60	0.0853508	52.06032
475001	475.001	35.5099	70	0.1055099	50.11731
450114	450.114	28.431	80	0.108431	48.80631
350447	350.447	27.5303	90	0.1175303	41.18814
264240	264.24	28.6671	110	0.1386671	36.64139
242073	242.073	21.7593	120	0.1417593	34.3161
200368	200.368	27.3433	130	0.1573433	31.52656
185120	185.12	23.4174	140	0.1634174	30.25183
-121455	-121.455	0	0	0	0

Table B. 2: Axial load and moment for SRC3

Force(N)	Force(KN)	Δ(mm)	e(mm)	e+Δ(m)	M=F(e+Δ)
1.24E+06	1241.46	0	0	0	0
1.13E+06	1130.21	14.6721	20	0.0346721	39.18675
950174	950.174	25.64	30	0.05564	52.86768
903278	903.278	20.2983	40	0.0602983	54.46613
709418	709.418	29.8352	50	0.0798352	56.63653
598911	598.911	35.7446	60	0.0957446	57.34246
535418	535.418	32.3625	70	0.1023625	54.80673
521057	521.057	22.2835	80	0.1022835	53.29551
413668	413.668	18.0865	90	0.1080865	44.71193
315587	315.587	14.9862	110	0.1249862	39.44402
301968	301.968	9.76636	120	0.1297664	39.18529
242927	242.927	5.79505	130	0.1357951	32.98828
226382	226.382	3.54873	140	0.1435487	32.49685
-111432	-111.432	0	0	0	0

Table B. 3: Axial load and moment for SRC4

Force(N)	Force(KN)	Δ(mm)	e(mm)	e+Δ(m)	M=F(e+Δ)
1387770	1387.77	0	0	0	0
1231890	1231.89	11.2688	10	0.0212688	26.20082
1.10E+06	1100.53	16.449	20	0.036449	40.11322
886007	886.007	27.1252	30	0.0571252	50.61329
814720	814.72	23.308	40	0.063308	51.57829
642204	642.204	27.8115	50	0.0778115	49.97088
594078	594.078	23.2253	60	0.0832253	49.44232
485810	485.81	25.7842	70	0.0957842	46.53292
440317	440.317	24.6457	80	0.1046457	46.07728
384057	384.057	26.77	90	0.11677	44.84634
315906	315.906	25.9516	110	0.1359516	42.94793
291530	291.53	25.3945	120	0.1453945	42.38686
262052	262.052	23.8416	130	0.1538416	40.3145
242000	242	23.1216	140	0.1631216	39.47543
-133217	-133.217	0	0	0	0

Table B. 4: Axial load and moment for SRC5

Force(N)	Force(KN)	Δ(mm)	e(mm)	e+Δ(m)	M=F(e+Δ)
1375620	1375.62	0	0	0	0
1231360	1231.36	12.2334	10	0.0222334	27.37732
1153800	1153.8	16.8017	20	0.0368017	42.4618
890214	890.214	28.8076	30	0.0588076	52.35135
855754	855.754	21.9611	40	0.0619611	53.02346
655715	655.715	35.6706	50	0.0856706	56.1755
630721	630.721	28.1617	60	0.0881617	55.60544
491122	491.122	36.7945	70	0.1067945	52.44913
468267	468.267	30.8755	80	0.1108755	51.91934
365745	365.745	34.5857	90	0.1245857	45.5666
273156	273.156	32.9393	110	0.1429393	39.04473
255395	255.395	27.1208	120	0.1471208	37.57392
206394	206.394	27.8321	130	0.1578321	32.5756
192307	192.307	24.357	140	0.164357	31.607
-124525	-124.525		0	0	0

Table B. 5: Axial load and moment for SRC6

Force(N)	Force(KN)	Δ(mm)	e(mm)	e+Δ(m)	M=F(e+Δ)
1275910	1275.91	0	0	0	0
1.17E+06	1165.8	14.8354	20	0.0348354	40.61111
952082	952.082	23.7526	30	0.0537526	51.17684
915641	915.641	16.8469	40	0.0568469	52.05135
730371	730.371	25.7827	50	0.0757827	55.34952
715316	715.316	17.4614	60	0.0774614	55.40938
555728	555.728	33.5066	70	0.1035066	57.5215
545674	545.674	25.236	80	0.105236	57.42455
410284	410.284	27.6198	90	0.1176198	48.25752
329205	329.205	15.4199	110	0.1254199	41.28886
311029	311.029	7.83727	120	0.1278373	39.7611
253644	253.644	12.2491	130	0.1422491	36.08063
241028	241.028	8.68305	140	0.1486831	35.83678
202099	202.099	4.28971	150	0.1542897	31.1818
-116254	-116.254	0	0	0	0

Table B. 6: Axial load and moment for RRC1

Force(N)	Force(KN)	Δ(mm)	e(mm)	e+Δ(m)	M=F(e+Δ)
1306380	1306.38	0	0	0	0
1208510	1208.51	7.77002	7.5	0.01527	18.45397
1109610	1109.61	12.9195	15	0.0279195	30.97976
881303	881.303	19.4652	25	0.0444652	39.18731
776823	776.823	19.0024	35	0.0540024	41.95031
639096	639.096	21.8842	45	0.0668842	42.74542
565779	565.779	20.4826	55	0.0754826	42.70647
463506	463.506	23.2332	65	0.0882332	40.89662
410883	410.883	22.5203	75	0.0975203	40.06943
350937	350.937	24.4664	85	0.1094664	38.41581
260909	260.909	22.307	105	0.127307	33.21554
240640	240.64	21.3879	115	0.1363879	32.82038
218985	218.985	19.9829	125	0.1449829	31.74908
201998	201.998	18.5307	135	0.1535307	31.01289
168022	168.022	16.4376	145	0.1614376	27.12507
-163371	-163.371	0	0	0	0

Table B. 7: Axial load and moment for RRC2

Force(N)	Force(KN)	Δ(mm)	e(mm)	e+Δ(m)	M=F(e+Δ)
1279130	1279.13	0	0	0	0
1.23E+06	1227.88	9.72907	7.5	0.0172291	21.15523
1159900	1159.9	16.5388	15	0.0315388	36.58185
940910	940.91	23.7629	25	0.0487629	45.8815
852137	852.137	22.9706	35	0.0579706	49.39889
670692	670.692	33.8107	45	0.0788107	52.85771
616994	616.994	32.0898	55	0.0870898	53.73388
497812	497.812	34.8984	65	0.0998984	49.73062
454057	454.057	33.1346	75	0.1081346	49.09927
371304	371.304	37.4993	85	0.1224993	45.48448
299741	299.741	34.5754	105	0.1395754	41.83647
281751	281.751	30.0429	115	0.1450429	40.86598
245153	245.153	27.9737	125	0.1529737	37.50196
225071	225.071	23.539	135	0.158539	35.68253
-144674	-144.674	0	0	0	0

Table B. 8: Axial load and moment for RRC3

Force(N)	Force(KN)	Δ(mm)	e(mm)	e+Δ(m)	M=F(e+Δ)
1238760	1238.76	0	0	0	0
1162320	1162.32	13.2414	15	0.0282414	32.82554
977429	977.429	23.9993	25	0.0489993	47.89332
912706	912.706	18.6708	35	0.0536708	48.98566
736921	736.921	25.7824	45	0.0707824	52.16104
700023	700.023	19.8838	55	0.0748838	52.42038
533837	533.837	39.2771	65	0.1042771	55.66697
510000	510	31.4148	75	0.1064148	54.27155
398888	398.888	34.2749	85	0.1192749	47.57733
310948	310.948	29.8298	105	0.1348298	41.92506
292304	292.304	25.0755	115	0.1400755	40.94463
248339	248.339	24.8275	125	0.1498275	37.20801
230187	230.187	20.4733	135	0.1554733	35.78793
196725	196.725	20.522	145	0.165522	32.56232
-92619.5	-92.6195	0	0	0	0

Table B. 9: Axial load and moment for RRC4

Force(N)	Force(KN)	Δ(mm)	e(mm)	e+Δ(m)	M=F(e+Δ)
1336370	1336.37	0	0	0	0
1.25E+06	1254.24	7.57903	7.5	0.015079	18.91272
1.15E+06	1150.76	12.7312	15	0.0277312	31.91196
891025	891.025	20.7295	25	0.0457295	40.74613
813048	813.048	19.8283	35	0.0548283	44.57804
651018	651.018	23.1832	45	0.0681832	44.38849
584045	584.045	20.2002	55	0.0752002	43.9203
480147	480.147	22.4484	65	0.0874484	41.98809
420537	420.537	21.0839	75	0.0960839	40.40684
367773	367.773	23.6111	85	0.1086111	39.94423
296456	296.456	22.5974	105	0.1275974	37.82701
271840	271.84	20.3606	115	0.1353606	36.79643
251441	251.441	18.349	125	0.143349	36.04382
230316	230.316	16.5431	135	0.1515431	34.9028
202131	202.131	14.601	145	0.159601	32.26031
-183731	-183.731	0	0	0	0

Table B. 10: Axial load and moment for RRC5

Force(N)	Force(KN)	Δ(mm)	e(mm)	e+Δ(m)	M=F(e+Δ)
1.33E+06	1327.52	0	0	0	0
1.26E+06	1256.65	11.1386	7.5	0.0186386	23.4222
1.18E+06	1179.65	13.9129	15	0.0289129	34.1071
954726	954.726	20.2896	25	0.0452896	43.23916
867721	867.721	19.2487	35	0.0542487	47.07274
684073	684.073	30.3686	45	0.0753686	51.55762
629967	629.967	27.9255	55	0.0829255	52.24033
500122	500.122	35.8833	65	0.1008833	50.45396
460533	460.533	33.0506	75	0.1080506	49.76087
373077	373.077	36.9279	85	0.1219279	45.4885
291422	291.422	34.8771	105	0.1398771	40.76326
269536	269.536	28.842	115	0.143842	38.7706
239516	239.516	28.3821	125	0.1533821	36.73747
215354	215.354	22.5185	135	0.1575185	33.92224
197155	197.155	22.7225	145	0.1677225	33.06733
-152091	-152.091	0	0	0	0

Table B. 11: Axial load and moment for RRC6

Force(N)	Force(KN)	Δ(mm)	e(mm)	e+Δ(m)	M=F(e+Δ)
1.27E+06	1268.92	0	0	0	0
1.19E+06	1186.05	13.3246	15	0.0283246	33.59439
1.00E+06	1001.9	20.1291	25	0.0451291	45.21485
925080	925.08	16.7	35	0.0517	47.82664
760105	760.105	21.0365	45	0.0660365	50.19467
710281	710.281	16.9799	55	0.0719799	51.12596
550523	550.523	31.559	65	0.096559	53.15795
535314	535.314	23.8709	75	0.0988709	52.92698
410189	410.189	30.1198	85	0.1151198	47.22088
310645	310.645	20.5328	105	0.1255328	38.99614
285312	285.312	15.5635	115	0.1305635	37.25133
240395	240.395	21.0946	125	0.1460946	35.12041
224913	224.913	18.0895	135	0.1530895	34.43182
200558	200.558	20.8695	145	0.1658695	33.26646
-144458	-144.458	0	0	0	0

APPENDIX C

ABAQUS OUTPUT OF LOAD -DISPLACEMENT CURVES

C.1 Load-displacement curve for SRC1

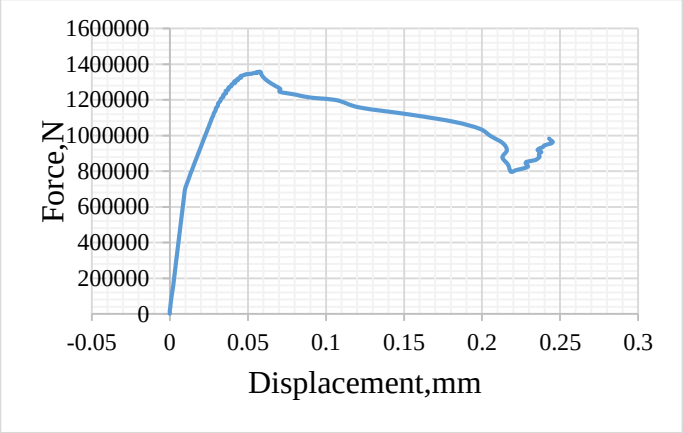

Figure C. 1: Force-displacement curve at, e=0

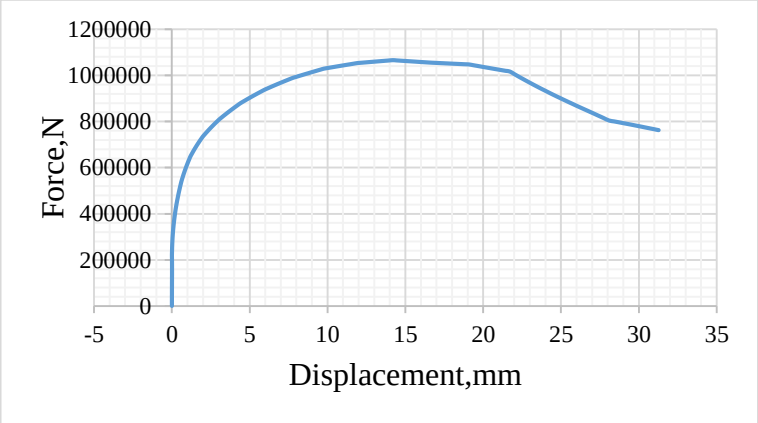

Figure C. 2: Force-displacement curve at, e=20

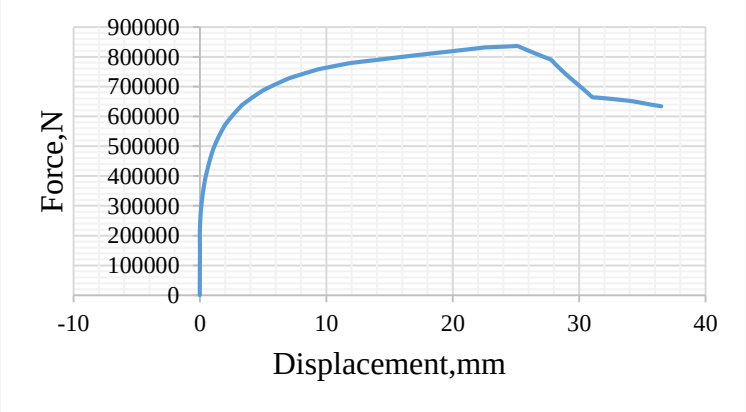

Figure C. 3: Force-displacement curve at, e=30

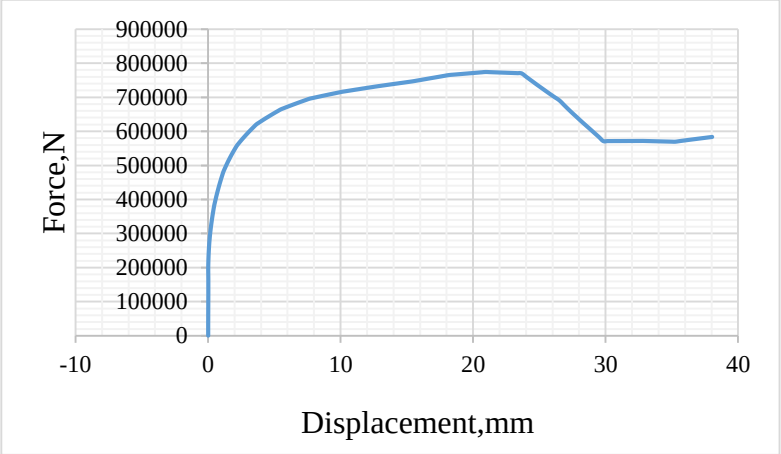

Figure C. 4: Force-displacement curve at, e=40

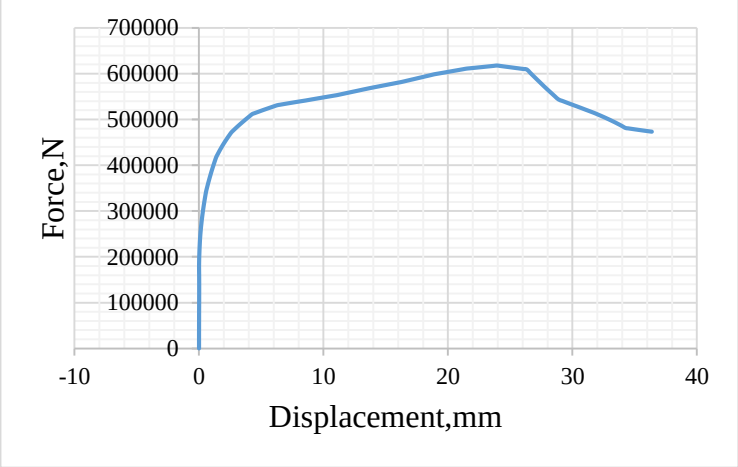

Figure C. 5: Force-displacement curve at, e=50

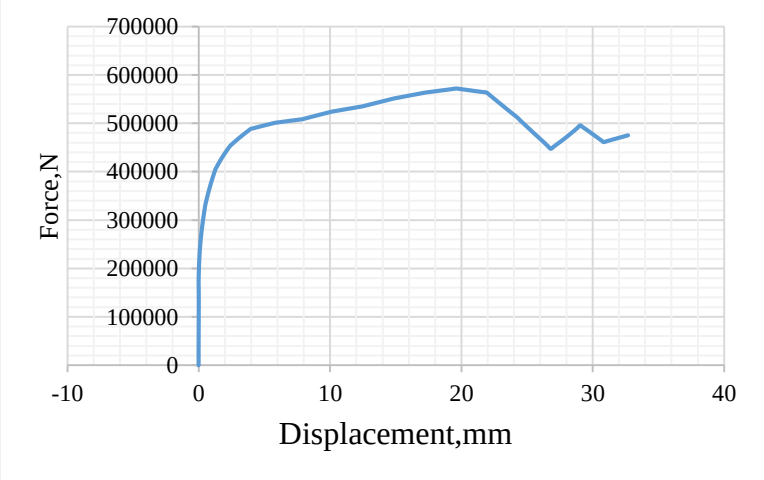

Figure C. 6: Force-displacement curve at, e=60

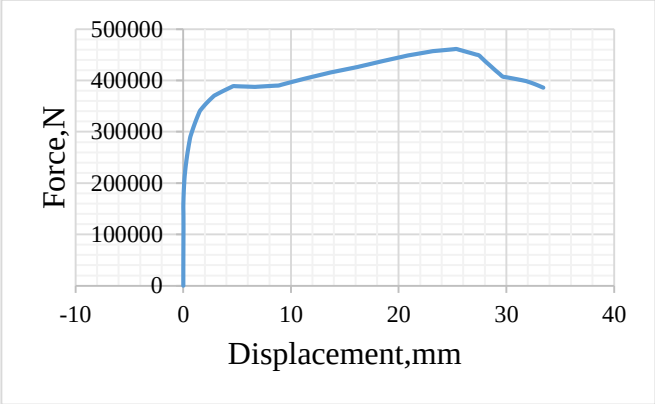

Figure C. 7: Force-displacement curve at, e=70

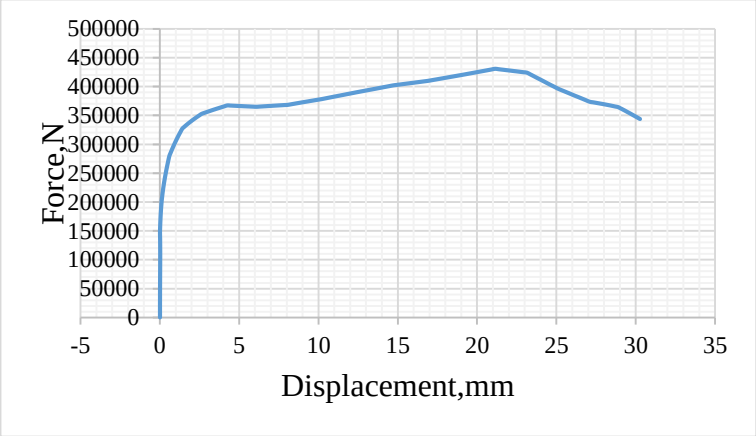

Figure C. 8: Force-displacement curve at, e=80

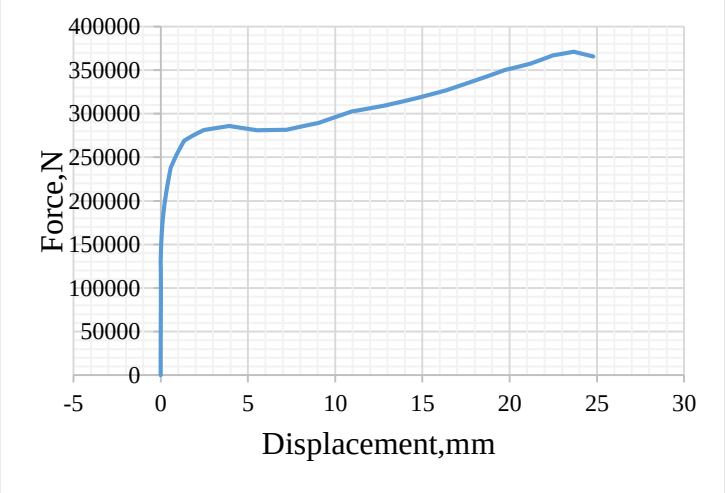

Figure C. 9: Force-displacement curve at, e=90

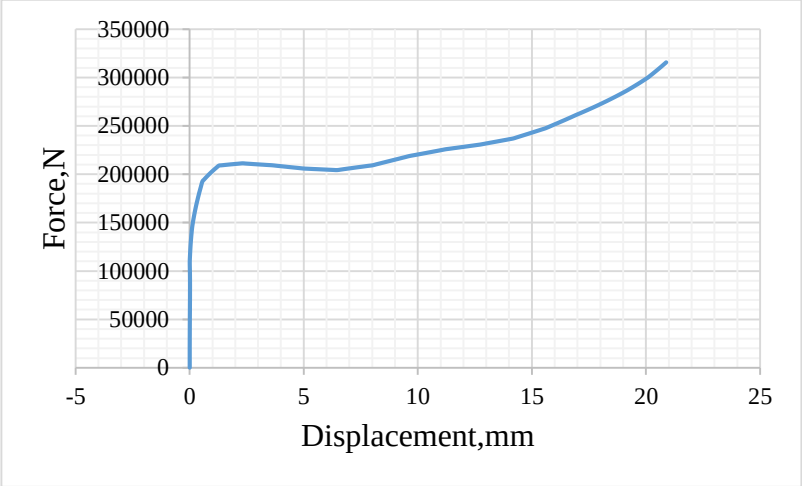

Figure C. 10: Force-displacement curve at, e=110

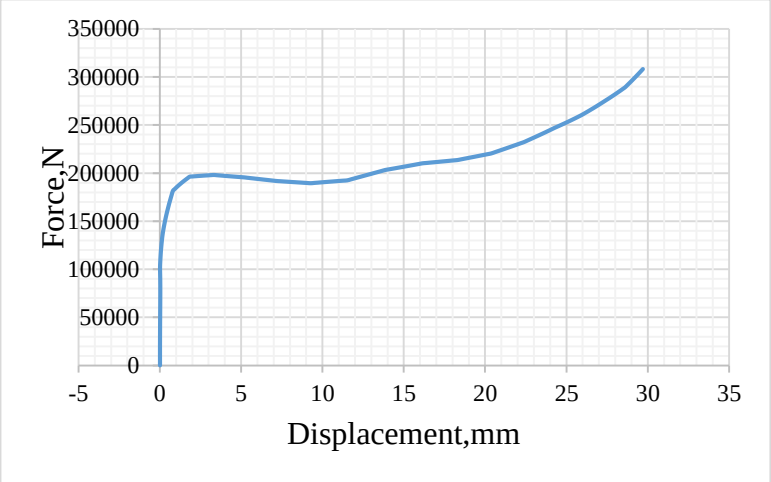

Figure C. 11: Force-displacement curve at, e=120

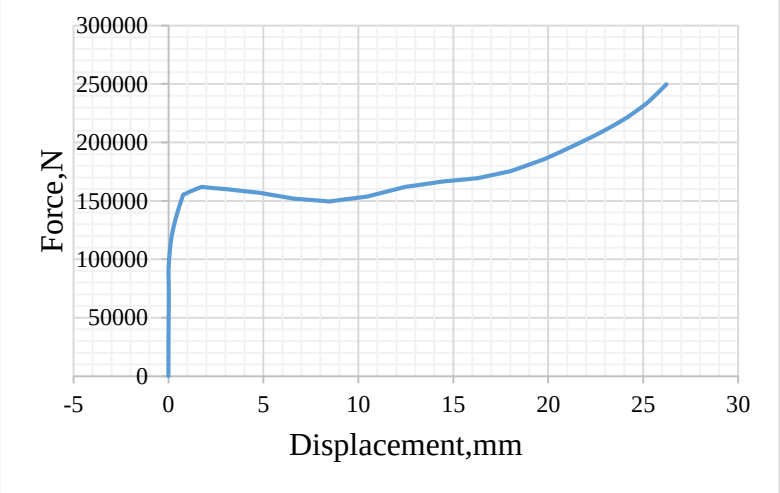

Figure C. 12: Force-displacement curve at, e=130

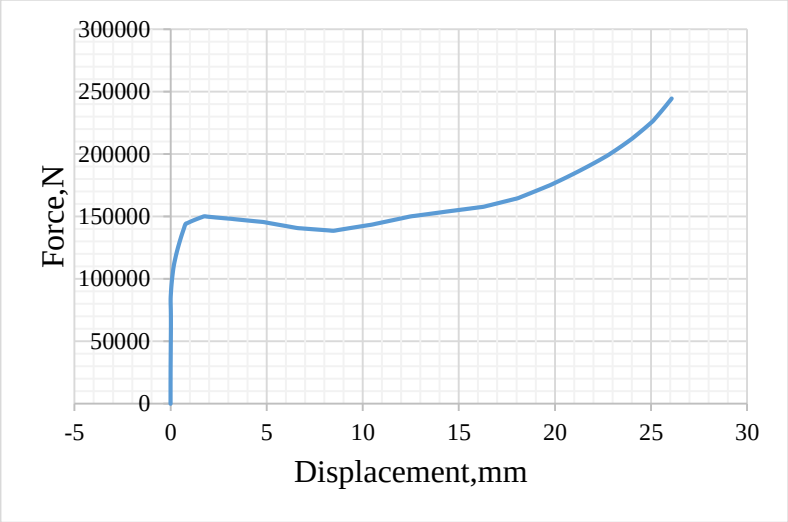

Figure C. 13: Force-displacement curve at, e=140

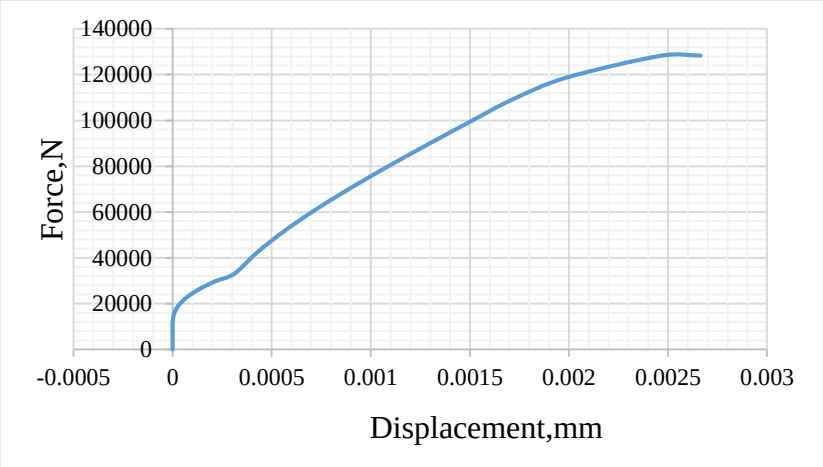

Figure C. 14: Tensile force- longitudinal displacement curve at, e=0

APPENDIX D

COMPARISON OF AXIAL LOAD AND MOMENT INTERACTION DIAGRAMS

D.1 Comparison based on slenderness ratio for rectangular RC column

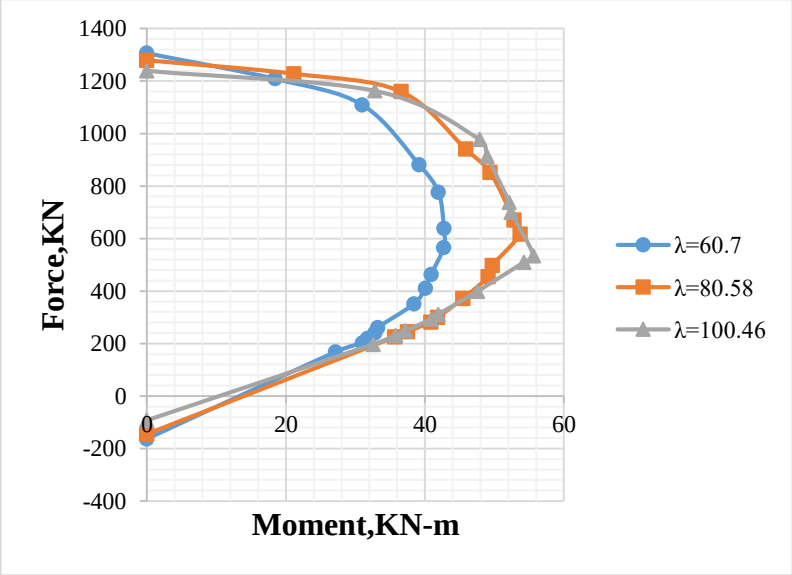

a) For ρ=0.01223

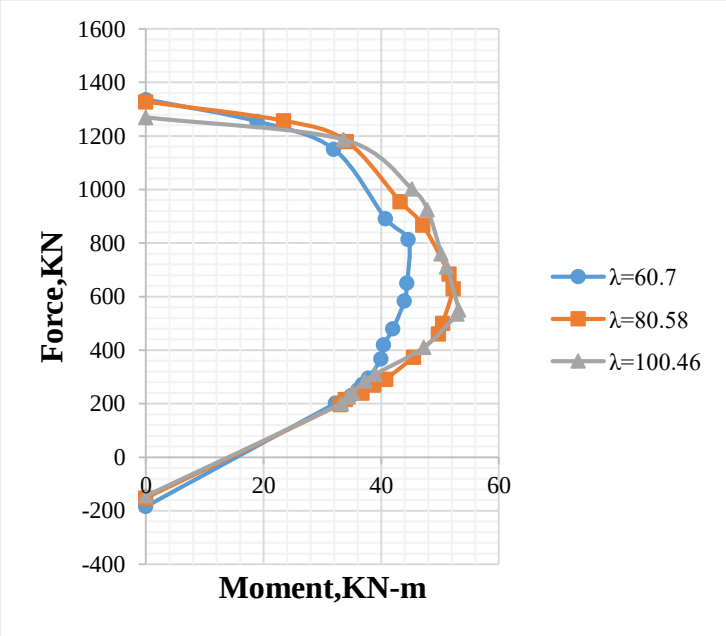

b) For ρ=0.0166

Figure D. 1: Comparison of Axial load-moment interaction diagram based on slenderness ratio.

D.2 Comparison based on steel ratio for rectangular RC column

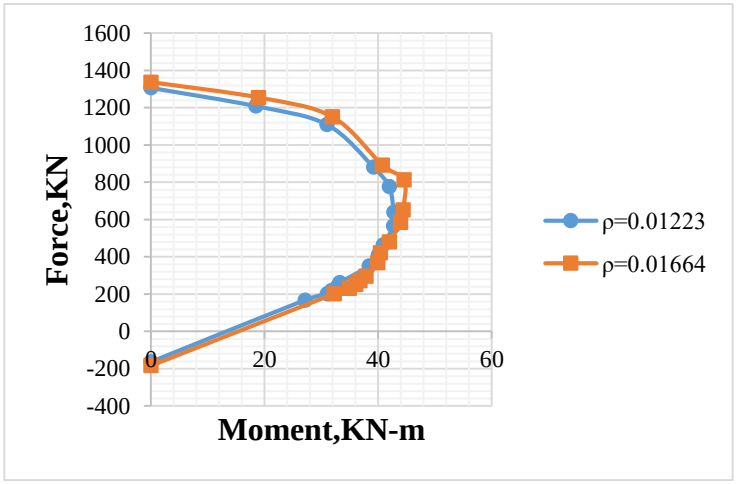

a) For λ=60.7

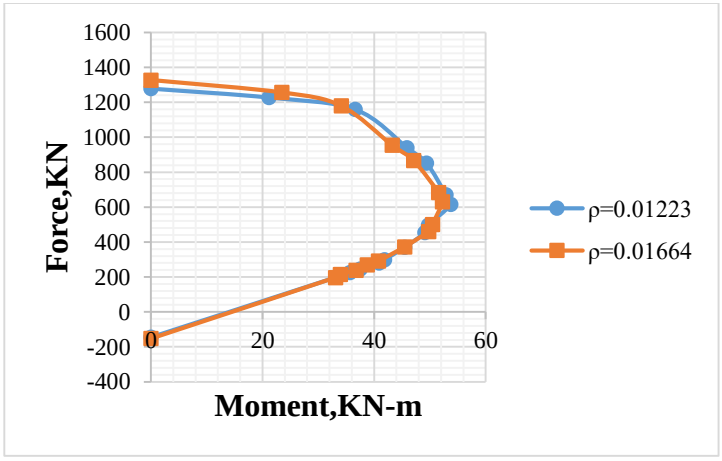

b) For λ=80.58

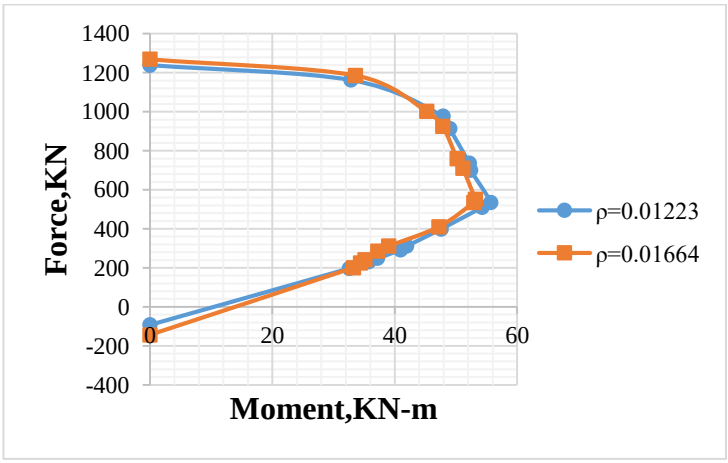

c) For λ=100.46

Figure D. 2: Comparison of Axial load-moment interaction diagram based on steel ratio.

D.3 Comparison based on shape of the column for ρ=0.0166

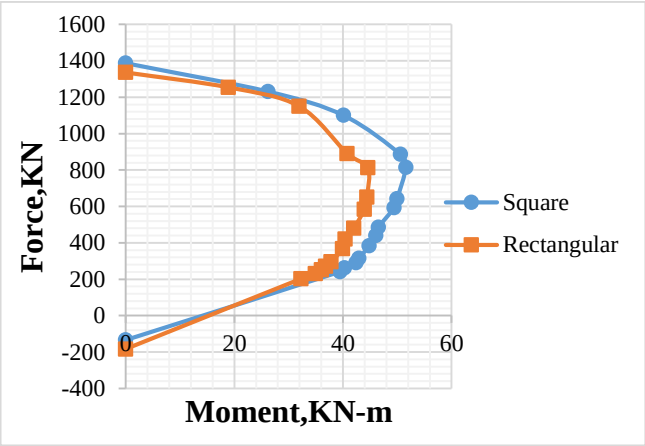

a) For λ=60.7

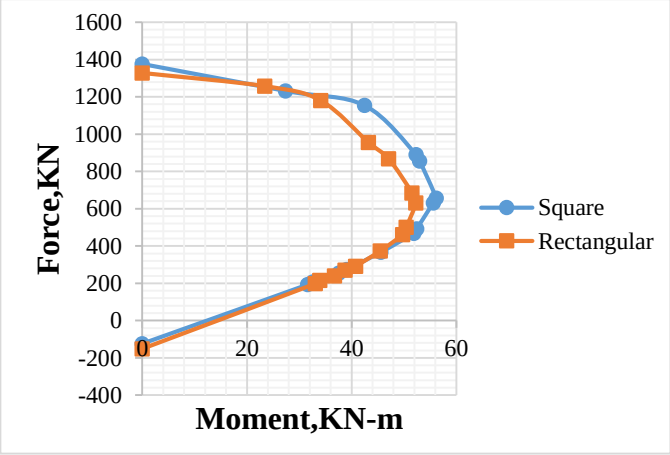

b) For λ=80.58

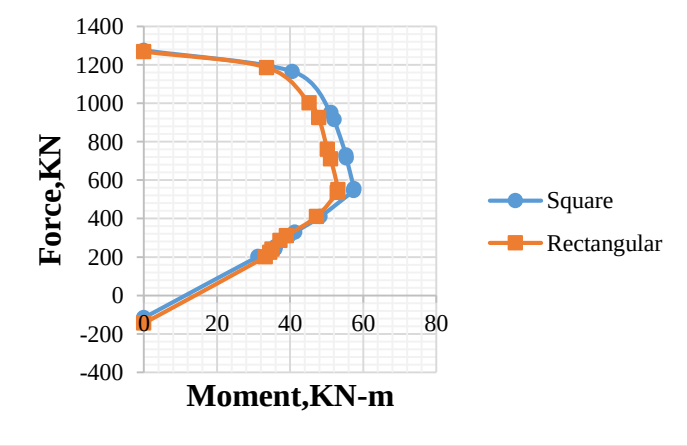

c) For λ=100.46

Figure D. 3: Comparison of Axial load-moment interaction diagram based on shape.

D.4 Comparison of FEA axial load-moment interaction diagram with Nominal stiffness method(NSM)

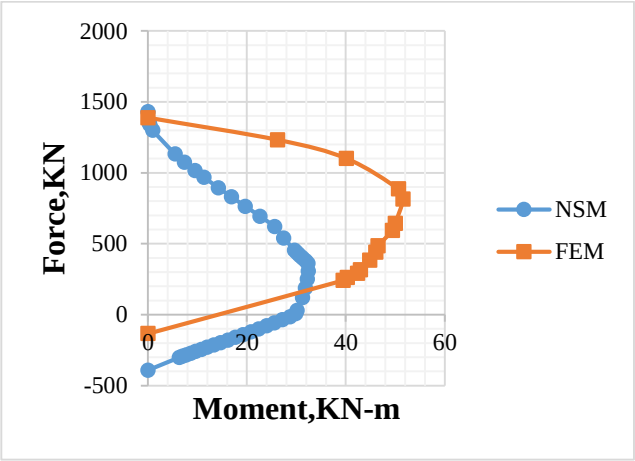

Figure D. 4: Comparison of FEA with NSM for SRC4

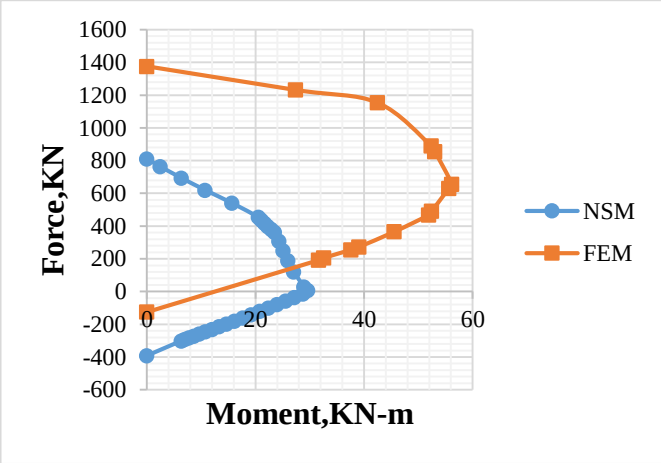

Figure D. 5: Comparison of FEA with NSM for SRC5

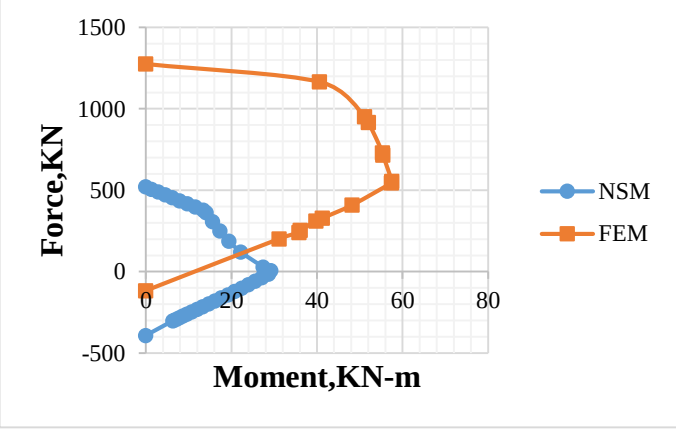

Figure D. 6: Comparison of FEA with NSM for SRC6

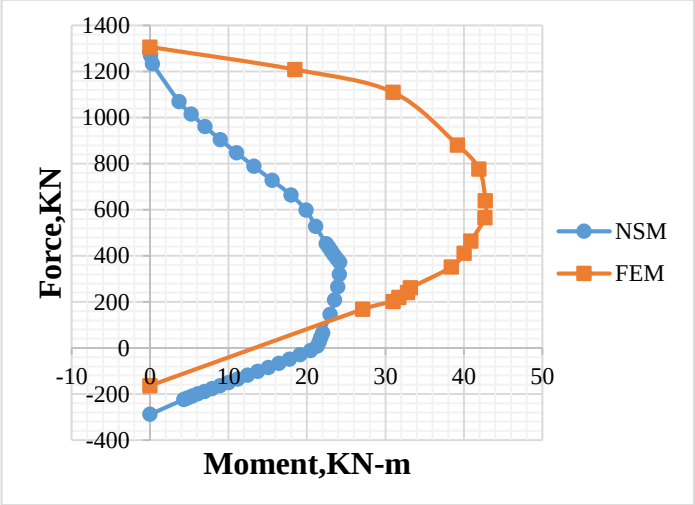

Figure D. 7: Comparison of FEA with NSM for RRC1

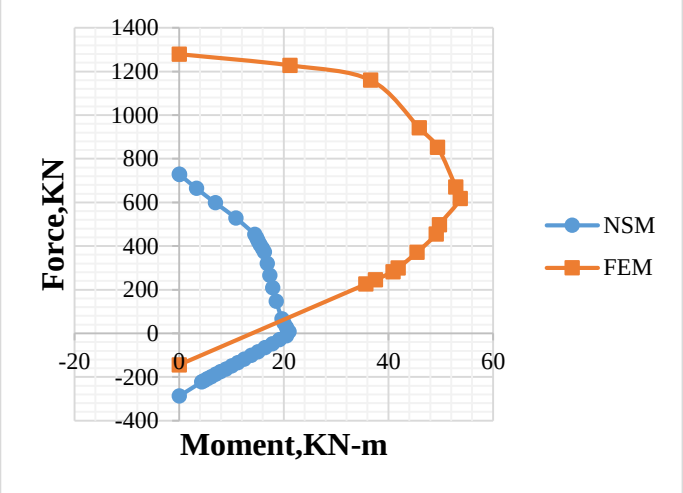

Figure D. 8: Comparison of FEA with NSM for RRC2

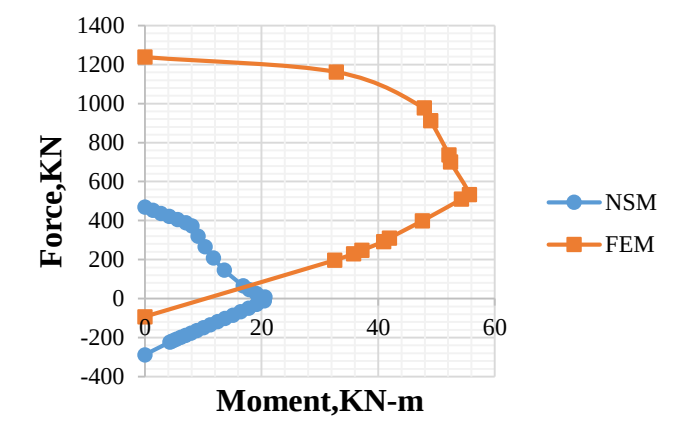

Figure D. 9: Comparison of FEA with NSM for RRC3

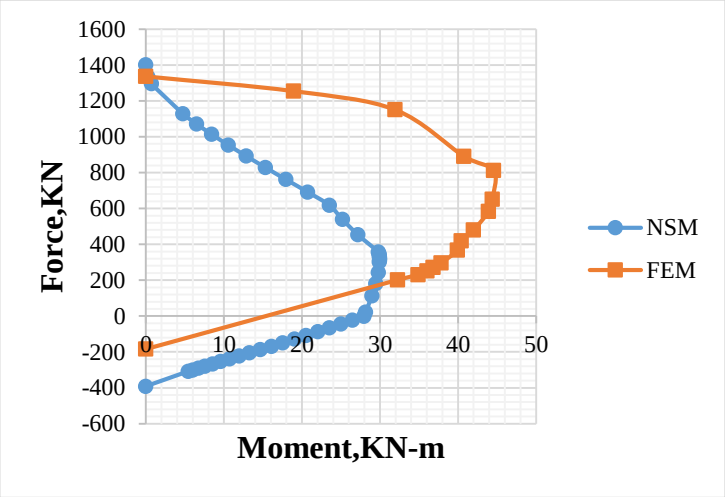

Figure D. 10: Comparison of FEA with NSM for RRC4

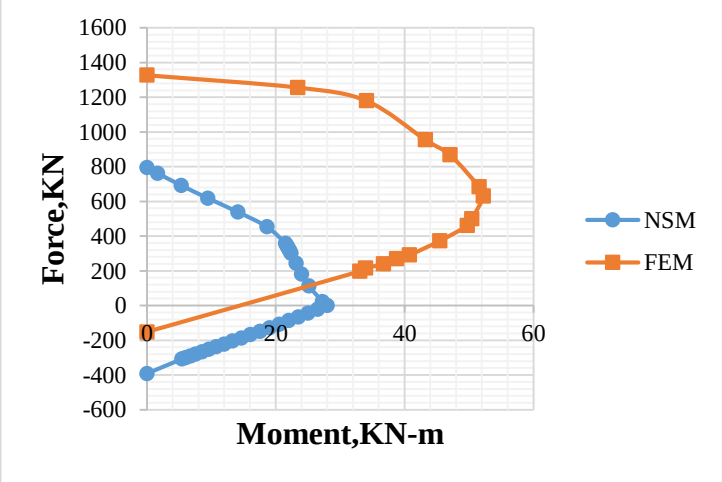

Figure D. 11: Comparison of FEA with NSM for RRC5

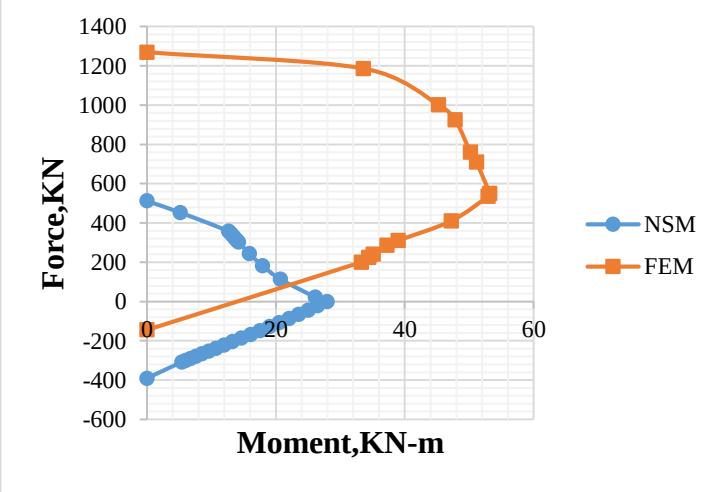

Figure D. 12: Comparison of FEA with NSM for RRC6